

EXPERIMENTAL INVESTIGATION OF $\text{CF}_3\text{I-CO}_2$ GAS MIXTURES ON THE BREAKDOWN CHARACTERISTICS IN UNIFORM AND NON- UNIFORM FIELD CONFIGURATIONS

A thesis submitted to Cardiff University

in candidature for the degree of

Doctor of Philosophy

By

MUHAMMAD SAUFI KAMARUDIN

School of Engineering

Cardiff University

June 2013

SUMMARY

This thesis is concerned with the investigation of trifluoroiodomethane (CF₃I) gas mixtures as an alternative for an insulation medium in high voltage applications. The work has involved a broad review of literature, followed by developing a test rig for carrying out experimental investigations, extensive computational modelling and simulation studies as well as extensive laboratory tests on CF₃I gas and its gas mixtures.

The literature survey reviewed the current trend of efforts taken by researchers to find solutions for minimizing the usage of sulphur hexafluoride (SF₆) as a gas insulator, focusing on CF₃I and its mixtures. The physical properties of CF₃I are investigated, along with thermal and electrical properties.

A new test rig has been designed and constructed specifically to be used for gas insulation research. The test rig is integrated with wireless temperature and humidity sensors, as well as an electrode gap length control system. The test rig is completed with a gas recovery system to ensure proper gas handling is carried out after each test.

Extensive laboratory experimental investigations on CF₃I mixtures have been completed, focusing on the mixture of CF₃I-CO₂ gas with a ratio of 30%-70%. Standard lightning impulse of 1.2/50 has been used, with both positive and negative polarity. The effects of electrode configuration, impulse polarity, electrode gap length, gas pressure, and CF₃I content have been investigated. Insulation properties such as 50% breakdown voltage (U_{50}) and $V-t$ characteristics for each test condition are investigated and presented, as well as the electric field behaviour. Finite element method (FEM) has been used to determine the electric field behaviour of a given test condition. This study revealed that CF₃I gas mixtures perform better under more uniform field condition. It was also found that an increase in gas pressure will increase the insulation strength and an increase in CF₃I content is more likely to give benefit in conditions with a more uniform field when compared to less uniform field conditions. Also, relation between liquefaction temperatures of a CF₃I-CO₂ mixture with varying CF₃I content has been developed for various pressures based on literature.

Observations on solid by-products of CF₃I have also been carried out. It has been found that iodine particles are deposited on both high voltage and ground electrodes, which can affect the insulation properties of CF₃I and its mixtures.

LIST OF CONTENTS

ACKNOWLEDGEMENTS	i
PUBLICATIONS	ii
SUMMARY	iii
LIST OF FIGURES	ix
LIST OF TABLES	xvi

CHAPTER 1:INTRODUCTION

1.1 BACKGROUND.....	1-1
1.2 DIRECTION OF RESEARCH AND OBJECTIVES	1-4
1.3 CONTRIBUTION OF THESIS	1-5
1.4 ORGANIZATION OF THESIS.....	1-6

CHAPTER 2:CF₃I MIXTURES AS SF₆ ALTERNATIVE: A REVIEW

2.1 INTRODUCTION	2-1
2.2 SULPHUR HEXAFLUORIDE (SF ₆) AS AN INSULATION GAS	2-1
2.3 PROPERTIES REQUIRED FOR POWER SYSTEM APPLICATIONS.....	2-3
2.3.1 <i>Circuit breaker applications</i>	2-3
2.3.2 <i>Gas-insulated transmission lines (GIL) applications</i>	2-4
2.3.3 <i>Gas-insulated transformers applications</i>	2-4
2.4 PHYSICAL AND CHEMICAL PROPERTIES OF CF ₃ I.....	2-5
2.4.1 <i>Electron Interaction Properties</i>	2-8

2.5	THERMAL PROPERTIES OF CF ₃ I.....	2-11
2.6	ELECTRICAL PROPERTIES OF CF ₃ I AND ITS MIXTURES.....	2-15
2.6.1	<i>50% Breakdown Voltage (U₅₀).....</i>	<i>2-15</i>
2.6.2	<i>V-t characteristics</i>	<i>2-18</i>
2.6.3	<i>Other electrical properties for CF₃I and its mixtures</i>	<i>2-22</i>
2.7	BY-PRODUCTS OF CF ₃ I.....	2-24
2.8	REDUCING THE BY-PRODUCTS OF CF ₃ I.....	2-26
2.9	TOXICITY OF CF ₃ I AND ITS BY-PRODUCTS.....	2-28
2.10	CONCLUSION.....	2-32

CHAPTER 3: PURPOSE-BUILT TEST RIG: DESIGN PRINCIPLES AND CONSTRUCTION DETAILS

3.1	INTRODUCTION	3-1
3.2	DESIGN OF THE PRESSURE VESSEL.....	3-1
3.2.1	<i>Structure.....</i>	<i>3-1</i>
3.2.2	<i>Materials.....</i>	<i>3-4</i>
3.3	ELECTRODES.....	3-6
3.4	LINEAR ACTUATOR.....	3-8
3.4.1	<i>Linear Actuator Main Unit</i>	<i>3-8</i>
3.4.2	<i>Linear Actuator Controller.....</i>	<i>3-9</i>
3.5	FITTINGS AND ASSEMBLIES	3-10
3.5.1	<i>Gauges</i>	<i>3-10</i>
3.5.2	<i>Hose, Valves and Hose Tails.....</i>	<i>3-10</i>
3.5.3	<i>Pressure Relief Valve.....</i>	<i>3-11</i>
3.6	BUSHING.....	3-12

3.7	TEMPERATURE AND HUMIDITY SENSOR	3-13
3.8	COMPRESSION SEAL FITTING	3-14
3.9	REGULATORS AND HEATER	3-16
3.10	GAS REMOVAL SYSTEM.....	3-17
3.11	GAS EVACUATION AND FILLING SYSTEM	3-20
3.12	GENERATION AND MEASUREMENT OF A LIGHTNING IMPULSE	3-22
3.12.1	<i>Generation of a Lightning Impulse.....</i>	3-23
3.12.2	<i>Measurement of Lightning Impulse.....</i>	3-25
3.12.3	<i>Recording Instrument.....</i>	3-26
3.13	CONCLUSION.....	3-27

**CHAPTER 4:SIMULATION MODEL AND FUNDAMENTAL MEASUREMENT
TECHNIQUES ON AIR BREAKDOWN UNDER LIGHTNING IMPULSE**

4.1	INTRODUCTION	4-1
4.2	FINITE ELEMENT MODELLING.....	4-2
4.2.1	<i>Simulated Model.....</i>	4-3
4.2.2	<i>Material Properties</i>	4-4
4.2.3	<i>Boundary Conditions.....</i>	4-5
4.2.4	<i>Mesh.....</i>	4-6
4.2.5	<i>Solver Settings.....</i>	4-7
4.3	ATMOSPHERIC CORRECTIONS IN DRY TESTS	4-7
4.3.1	<i>Atmospheric Correction Factors for Air Gaps</i>	4-8
4.4	EXPERIMENTAL CHARACTERISATION OF ON AIR BREAKDOWN.....	4-13
4.4.1	<i>Effect of Gap Length and Pressure</i>	4-14
4.4.2	<i>Effects of Electrode Configuration.....</i>	4-21

4.5 CONCLUSION.....	4-28
---------------------	------

**CHAPTER 5: BREAKDOWN PROPERTIES OF CF₃I AND ITS MIXTURES
UNDER LIGHTNING IMPULSE: EFFECT OF GAP GEOMETRY AND
IMPULSE POLARITY**

5.1 INTRODUCTION	5-1
5.2 CALCULATION OF CF ₃ I-CO ₂ MIXTURES.....	5-2
5.3 EFFECTS OF ELECTRODE CONFIGURATION AND IMPULSE POLARITY	5-5
5.3.1 Magnitude of U_{50} and E_{max}	5-10
5.3.2 <i>V-t Characteristics</i>	5-14
5.4 EFFECTS OF GAP LENGTH.....	5-15
5.4.1 <i>Rod-plane Electrode Configuration</i>	5-16
5.4.2 <i>Plane-plane Electrode Configuration</i>	5-20
5.4.3 <i>Sphere Gap Electrode Configuration</i>	5-25
5.5 CONCLUSION.....	5-30

**CHAPTER 6: BREAKDOWN PROPERTIES OF CF₃I AND ITS MIXTURES
UNDER LIGHTNING IMPULSE: EFFECTS OF GAS PRESSURE AND CF₃I
CONTENT**

6.1 INTRODUCTION	6-1
6.2 EFFECT OF GAS PRESSURE.....	6-2
6.2.1 Magnitude of U_{50} and E_{max}	6-2
6.2.2 <i>V-t Characteristics</i>	6-8
6.3 EFFECT OF CF ₃ I CONTENT	6-13

6.3.1	<i>Effects of CF₃I Content in a Rod-Plane Electrode Configuration</i>	6-14
6.3.2	<i>Effects of CF₃I Content in Plane-Plane Electrode Configuration</i>	6-21
6.3.3	<i>Relation of CF₃I Content with Liquefaction Temperature (T_{mb})</i>	6-28
6.4	OBSERVATION ON SOLID BY-PRODUCTS OF CF ₃ I-CO ₂ MIXTURES.....	6-32
6.5	CONCLUSION.....	6-39

CHAPTER 7:GENERAL CONCLUSIONS AND FUTURE WORKS

7.1	GENERAL CONCLUSIONS	7-1
7.2	FUTURE WORK.....	7-6

REFERENCES	i
-------------------------	----------

APPENDIX A	xi
-------------------------	-----------

APPENDIX B	xii
-------------------------	------------

LIST OF FIGURES

Figure 1.1: Simplified UK electrical power transmission system [1].....	1-2
Figure 2.1: 3D molecular drawing of CF ₃ I, showing three fluorine atoms (light blue) and an iodine atom (purple) connected to a carbon atom (grey) [25].....	2-5
Figure 2.2: Electron drift velocities as a function of E/N at different CF ₃ I ratio <i>k</i> in comparison with SF ₆ [33].....	2-9
Figure 2.3: Density-normalized effective ionization coefficients ($\alpha-\eta$)/N as a function of E/N at different CF ₃ I gas mixture ratio <i>k</i> in comparison with SF ₆ [33].....	2-10
Figure 2.4: The limiting field as a function of CF ₃ I and SF ₆ gas content <i>k</i> [33].....	2-10
Figure 2.5: Saturation vapour pressure curves for SF ₆ , CO ₂ , N ₂ , and CF ₃ I.....	2-12
Figure 2.6: Saturation vapour pressure curves for SF ₆ , CO ₂ , N ₂ , and CF ₃ I (0.1 MPa to 1.0 MPa).....	2-13
Figure 2.7: Saturation vapour pressure curves for CF ₃ I and SF ₆ as given by [39].....	2-14
Figure 2.8: U ₅₀ for CF ₃ I-CO ₂ mixtures [39].....	2-17
Figure 2.9: Breakdown (a) before and (b) after peak of lightning impulse	2-18
Figure 2.10: <i>V-t</i> characteristics at 0.1 MPa [45] under positive polarity. Dashed lines indicate U ₅₀ in Table 2.5	2-19
Figure 2.11: <i>V-t</i> characteristics at 0.1 MPa [45] under negative polarity. Dashed lines indicate U ₅₀ in Table 2.5	2-20
Figure 2.12: <i>V-t</i> characteristics for gap 10mm; positive polarity [47].....	2-21
Figure 2.13: <i>V-t</i> characteristics at 0.1 MPa [46].....	2-22
Figure 2.14: Interruption capabilities of CF ₃ I, CF ₃ I-N ₂ and CF ₃ -CO ₂ mixtures as compared to SF ₆ [39].....	2-23

Figure 2.15: Relation between C_2F_6 and amount of sparkover times with different electrodes [55]	2-24
Figure 2.16: Effects of by-products and deteriorated CF_3I on insulation performance of CF_3I [55].....	2-25
Figure 2.17: Iodine adsorption [41]	2-27
Figure 2.18: Iodine density after an interruption [42]	2-27
Figure 3.1: Pressure vessel	3-2
Figure 3.2: Bottom view of the pressure vessel	3-3
Figure 3.3: Structure with legs	3-4
Figure 3.4: Pressure vessel	3-6
Figure 3.5: Electrodes (radius in mm)	3-7
Figure 3.6: Firgelli linear actuator [76].....	3-9
Figure 3.7: Firgelli linear actuator dimensions (in mm) [76].....	3-9
Figure 3.8: Liner actuator controller – PhidgetAdvancedServo 1-Motor [77].....	3-9
Figure 3.9: Two types of gauges	3-10
Figure 3.10: Pressure relief valve	3-11
Figure 3.11: Bushing.....	3-13
Figure 3.12: Temperature and humidity sensor – main unit and remote unit	3-14
Figure 3.13: Sealing gland	3-15
Figure 3.14: Compressed air pressure regulator.....	3-16
Figure 3.15: CO_2 pressure regulator	3-16
Figure 3.16: CO_2 heater	3-17
Figure 3.17: DILO gas recovery system	3-18
Figure 3.18: DILO modules and function [82].....	3-19
Figure 3.19: Gas evacuation and filling system	3-22

Figure 3.20: Schematic diagram of impulse generator; R_{ch} (4.7 k Ω): charging resistor; R_s (12.1 Ω): front resistor; R_p (67 Ω): tail resistor; R_{pot} (0.78 M Ω): potential resistor; C_s (2.0 μ F): impulse capacitance; C_{load} =load capacitance [84]	3-23
Figure 3.21: Haefely SGSA impulse generator	3-24
Figure 3.22: Schematic diagram for charging unit; R1 (165 Ω): Demagnisation resistor; R2 (2.7 Ω): Primary damping resistor; R3 (8.5 Ω): High voltage damping resistor; R4 (200 M Ω) and R5 (5.5 M Ω): DC measuring resistors [85]	3-24
Figure 3.23: Impulse generator control unit.....	3-25
Figure 3.24: Capacitive voltage divider.....	3-25
Figure 3.25: Digital storage oscilloscope.....	3-26
Figure 3.26: Block diagram of the test rig	3-26
Figure 3.27: Standard 1.2/50 lightning impulse	3-27
Figure 4.1: General procedures for FEM simulations in COMSOL Multiphysics	4-3
Figure 4.2: A 2D- axis-symmetric model in COMSOL Multiphysics	4-4
Figure 4.3: Discretisation of the domain problem with mesh refinement at the region of interest (plane-electrode).....	4-7
Figure 4.4: Values of exponent m as a function of parameter g [44]	4-10
Figure 4.5: Values of exponent w as a function of parameter g [44].....	4-11
Figure 4.6: Flowchart for atmospheric corrections in dry tests.....	4-12
Figure 4.7: Three configurations of gap electrode for air breakdown tests	4-13
Figure 4.8: U_{50} for air breakdown in rod-plane gap as a function of pressure.....	4-14
Figure 4.9: Lines of electric field with equal magnitudes with maximum electric field region at the tip of the rod (kV/cm)	4-16
Figure 4.10: Electric field magnitude along the edge of the high voltage conductor (refer to Figure 4.9)	4-17

Figure 4.11: Electric field magnitude along the gap of the rod-plane electrode (refer to Figure 4.9).....	4-18
Figure 4.12: E/E_{\max} curve along the gap of the rod-plane electrode.....	4-18
Figure 4.13: E_{\max} for air breakdown in a rod-plane gap as a function of gap length...	4-19
Figure 4.14: U_{50} curve for air under rod-plane electrode configuration in relation to product of pressure and gap length, pd	4-20
Figure 4.15: E_{\max} curve for air under rod-plane electrode configuration in relation to product of pressure and gap length, pd	4-20
Figure 4.16: U_{50} for different electrode configurations	4-21
Figure 4.17: Lines of electric field with equal magnitudes with maximum electric field region at the edge of the electrode for plane-plane configuration (kV/cm).....	4-22
Figure 4.18: Lines of electric field with equal magnitudes with maximum electric field region at the edge of the electrode for a R12-plane configuration (kV/cm)	4-23
Figure 4.19: Electric field magnitude along the surface of the plane (energized) electrode in plane-plane configuration (refer to Figure 4.17).....	4-24
Figure 4.20: Electric field magnitude along the R12 electrode in R12-plane configuration (refer to Figure 4.18).....	4-25
Figure 4.21: Electric field magnitude along the gap of the R12-plane electrode (refer to Figure 4.18).....	4-25
Figure 4.22: U_{50} curve in relation to the product of pressure and gap length, pd , for all electrode configurations.....	4-27
Figure 4.23: E_{\max} curve in relation to the product of pressure and gap length, pd , for all electrode configurations.....	4-28
Figure 5.1: 1 kg CF_3I bottle.....	5-2
Figure 5.2: CF_3I description on the bottle.....	5-2

Figure 5.3: Three configurations of electrodes for CF ₃ I gas mixtures breakdown tests	5-6
Figure 5.4: Lines of electric field with equal magnitudes with maximum electric field region at the tip of the sphere gap configuration (kV/cm)	5-7
Figure 5.5: Electric field along the surface of high voltage sphere electrode (refer to Figure 5.4)	5-7
Figure 5.6: Electric field along the gap of sphere gap electrode (refer to Figure 5.4)	5-8
Figure 5.7: Effects of electrode configuration on CF ₃ I-CO ₂ (30%-70%) mixtures under positive and negative impulse polarities in a 1 cm gap	5-11
Figure 5.8: Relationship between U ₅₀ and E _{max} according to the electrode systems of CF ₃ I-CO ₂ (30%-70%) gas mixture under positive impulse polarities	5-13
Figure 5.9: Effects of field utilization factor on U ₅₀ of CF ₃ I-CO ₂ (30%-70%) gas mixture under positive impulse polarities	5-14
Figure 5.10: <i>V-t</i> characteristics for various electrode configurations; 1 cm gap	5-15
Figure 5.11: Effects of gap length on CF ₃ I-CO ₂ (30%-70%) gas mixtures in rod-plane electrode configuration under positive and negative impulse	5-18
Figure 5.12: <i>V-t</i> characteristics for CF ₃ I-CO ₂ (30%-70%); rod-plane electrode configuration	5-20
Figure 5.13: Effects of gap length on CF ₃ I-CO ₂ (30%-70%) mixtures in a plane-plane electrode configuration under positive and negative impulses	5-22
Figure 5.14: <i>V-t</i> characteristics for CF ₃ I-CO ₂ (30%-70%); plane-plane electrode configuration	5-24
Figure 5.15: Effects of gap length on CF ₃ I-CO ₂ (30%-70%) mixtures in a sphere gap electrode configuration under positive and negative impulses	5-26
Figure 5.16: <i>V-t</i> characteristics for CF ₃ I-CO ₂ (30%-70%); sphere gap electrode configuration for positive impulse and negative impulses	5-27

Figure 5.17: Curves for $\text{CF}_3\text{I-CO}_2$ (30%-70%) in all electrode configurations under both positive and negative lightning impulses in relation with gap length	5-29
Figure 6.1: Curves for various pressures in relation to gap length.....	6-4
Figure 6.2: Effects of $\text{CF}_3\text{I-CO}_2$ pressures on U_{50} in a rod-plane electrode	6-6
Figure 6.3: Effects of $\text{CF}_3\text{I-CO}_2$ pressures on E_{\max} in a rod-plane electrode.....	6-7
Figure 6.4: Effect of $\text{CF}_3\text{I-CO}_2$ pressures on $E_{\text{normalised}}$ in a rod-plane electrode.....	6-8
Figure 6.5: $V-t$ characteristics for $\text{CF}_3\text{I-CO}_2$ (30%-70%) with a rod-plane electrode configuration under a positive impulse.....	6-10
Figure 6.6: $V-t$ characteristics for $\text{CF}_3\text{I-CO}_2$ (30%-70%) mixture using a rod-plane electrode configuration under negative impulses at various pressures.....	6-12
Figure 6.7: U_{50} curve for $\text{CF}_3\text{I-CO}_2$ (30%-70%) mixtures under a rod-plane electrode configuration in relation to the product of pressure and gap length, pd	6-13
Figure 6.8: Curves for different $\text{CF}_3\text{I-CO}_2$ mixtures in rod-plane electrode configurations, under both positive and negative lightning impulses, as a function of gap length.....	6-16
Figure 6.9: Effects of CF_3I content in a rod-plane electrode configuration under positive and negative impulse polarities	6-18
Figure 6.10: $V-t$ characteristics for $\text{CF}_3\text{I-CO}_2$ gas mixtures in a rod-plane electrode configuration with 1 cm gap.....	6-20
Figure 6.11: Curves for different $\text{CF}_3\text{I-CO}_2$ mixtures in a plane-plane electrode configuration, under both positive and negative lightning impulses in relation to gap length.....	6-23
Figure 6.12: Effects of CF_3I content on in a plane-plane electrode configuration under positive and negative impulse polarities	6-25

Figure 6.13: $V-t$ characteristics for CF_3I-CO_2 mixtures in a plane-plane electrode configuration with a 1 cm gap	6-27
Figure 6.14: Relation of liquefaction temperature with CF_3I content at different gas pressures (Yamamoto method).....	6-29
Figure 6.15: Relation of liquefaction temperature to CF_3I content at different gas pressures (Duan method).....	6-31
Figure 6.16: Solid by-product on electrodes	6-33
Figure 6.17: Specimen bombarded with an electron beam (reproduced from [119]) .	6-34
Figure 6.18: Rod electrode placed on the SEM tray.....	6-34
Figure 6.19: View from one of the cameras inside the SEM	6-35
Figure 6.20: Electron image of (a) rod electrode, and (b) plane electrode	6-36
Figure 6.21: EDX spectrum on a rod electrode.....	6-36
Figure 6.22: EDX spectrum on a plane electrode.....	6-37
Figure 6.23: Surface condition of a PTFE insulator after flashover in CF_3I [47]	6-38

LIST OF TABLES

Table 2.1: Physical properties of CF ₃ I [26].....	2-6
Table 2.2: Lifetimes, radiative efficiencies and direct GWPs relative to CO ₂ [28]	2-7
Table 2.3: Breakdown strengths of selected gases relative to SF ₆ [23], [29].....	2-7
Table 2.4: Coefficients for Eqn. (2.1) [35].....	2-12
Table 2.5: 50% breakdown voltage, U ₅₀ , for SF ₆ and CF ₃ I gases at 0.1 MPa under steep front square voltage application [45].....	2-16
Table 2.6: Field utilization factors for different electrode configurations [47].....	2-21
Table 2.7: Toxicity review of SF ₆ , CO ₂ , Air, CF ₃ I and by-products of CF ₃ I [63], [64], [65], [66], [67], [68], [69] and [70].....	2-30
Table 3.1: Symbols used in EN 10025-2: 2004: Non-alloy structural steel [71]	3-5
Table 3.2: Bushing specifications.....	3-12
Table 3.3: Humidity and temperature sensor specifications [80].....	3-14
Table 3.4: Sealing gland specifications.....	3-15
Table 4.1: Properties of materials used for FEM modelling	4-5
Table 4.2: Values for exponents m for air density correction and w for humidity correction, as a function of the parameter g [44].....	4-11
Table 4.3: U ₅₀ for air breakdown in rod-plane configuration (kV)	4-14
Table 4.4: E _{max} for air breakdown in the rod-plane configuration (kV/cm)	4-19
Table 4.5: U ₅₀ for different electrode configurations (kV)	4-21
Table 4.6: E _{max} for different electrode configurations (kV/cm)	4-26
Table 4.7: Field utilization factors for each electrode configuration with V = 1 kV ..	4-27
Table 5.1: Field utilization factors for each electrode configuration with V = 1 kV ..	5-10

Table 5.2: U_{50} and E_{\max} of CF_3I-CO_2 mixtures for each electrode configuration with a 1 cm gap	5-11
Table 5.3: U_{50} and E_{\max} for CF_3I-CO_2 mixtures (30%-70%) in rod-plane gap	5-17
Table 5.4: U_{50} and E_{\max} for CF_3I-CO_2 mixtures (30%-70%) in a plane-plane gap	5-20
Table 5.5: U_{50} and E_{\max} for CF_3I-CO_2 mixtures (30%-70%) in a sphere gap	5-25
Table 6.1: Partial pressures of CF_3I and CO_2 gases for mixture ratio of 30%-70%.....	6-2
Table 6.2: U_{50} for CF_3I-CO_2 (30%-70%) Mixtures for Various Pressures.....	6-3
Table 6.3: E_{\max} for CF_3I-CO_2 (30%-70%) Mixtures for Various Pressures.....	6-3
Table 6.4: $E_{\text{normalised}}$ for CF_3I-CO_2 (30%-70%) Mixtures for Various Pressures.....	6-3
Table 6.5: U_{50} for different CF_3I content in CF_3I-CO_2 gas mixtures in rod-plane electrode configurations	6-14
Table 6.6: E_{\max} for different CF_3I content in CF_3I-CO_2 gas mixtures in a rod-plane electrode configuration	6-15
Table 6.7: $E_{\text{normalised}}$ for different CF_3I content in CF_3I-CO_2 gas mixtures in a rod-plane electrode configuration	6-15
Table 6.8: Effects of a 20% increase in CF_3I content on U_{50} and E_{\max} in a rod-plane electrode configuration under positive and negative impulse polarities.....	6-19
Table 6.9: U_{50} for different CF_3I content in CF_3I-CO_2 gas mixtures in a plane-plane electrode configuration	6-21
Table 6.10: E_{\max} for different CF_3I content in CF_3I-CO_2 gas mixtures in a plane-plane electrode configuration	6-21
Table 6.11: $E_{\text{normalised}}$ for different CF_3I content in CF_3I-CO_2 gas mixtures in a plane-plane electrode configuration	6-22
Table 6.12: Effects of 20% increase in CF_3I content on U_{50} and E_{\max} in a plane-plane electrode configuration under positive and negative impulse polarities.....	6-26

Table 6.13: Element analysis from an EDX spectrum on a rod electrode..... 6-36

Table 6.14: Element analysis from an EDX spectrum on a plane electrode..... 6-37

CHAPTER 1: INTRODUCTION

1.1 Background

The electrical power supply plays such an important role in today's modernized world that the quality and continuity of supply is of highest priority. Power producers have put enormous effort into ensuring demand for electricity is securely and reliably delivered to customers, ranging from a small power outlet in a house to a large processing plant. From the consumer's perspective, any interruptions to the electrical supply could be problematic, be it a blackout, voltage dip, or overvoltage that could contribute to loss of equipment, or disruption of service. In fact this could directly impact the economy as a whole, if on a large enough scale.

In a typical power system, there are three major parts, these include generation, transmission, and distribution of electricity. During generation, other sources of energy, such as wind, solar, water, and even nuclear, are converted into electrical power. The power is then transmitted in bulk by means of overhead lines or underground cables at a variety of levels which depend on the power generated, distance of transmission, loads condition at the end part and other factors. Voltage is typically increased significantly prior to transmission in order to reduce losses. The final stage of the delivery of electricity is distribution. Distribution usually involves a network of substations, again depending on the consumers' needs, these will be in different levels of rating. Figure 1.1 below shows an example of such system.

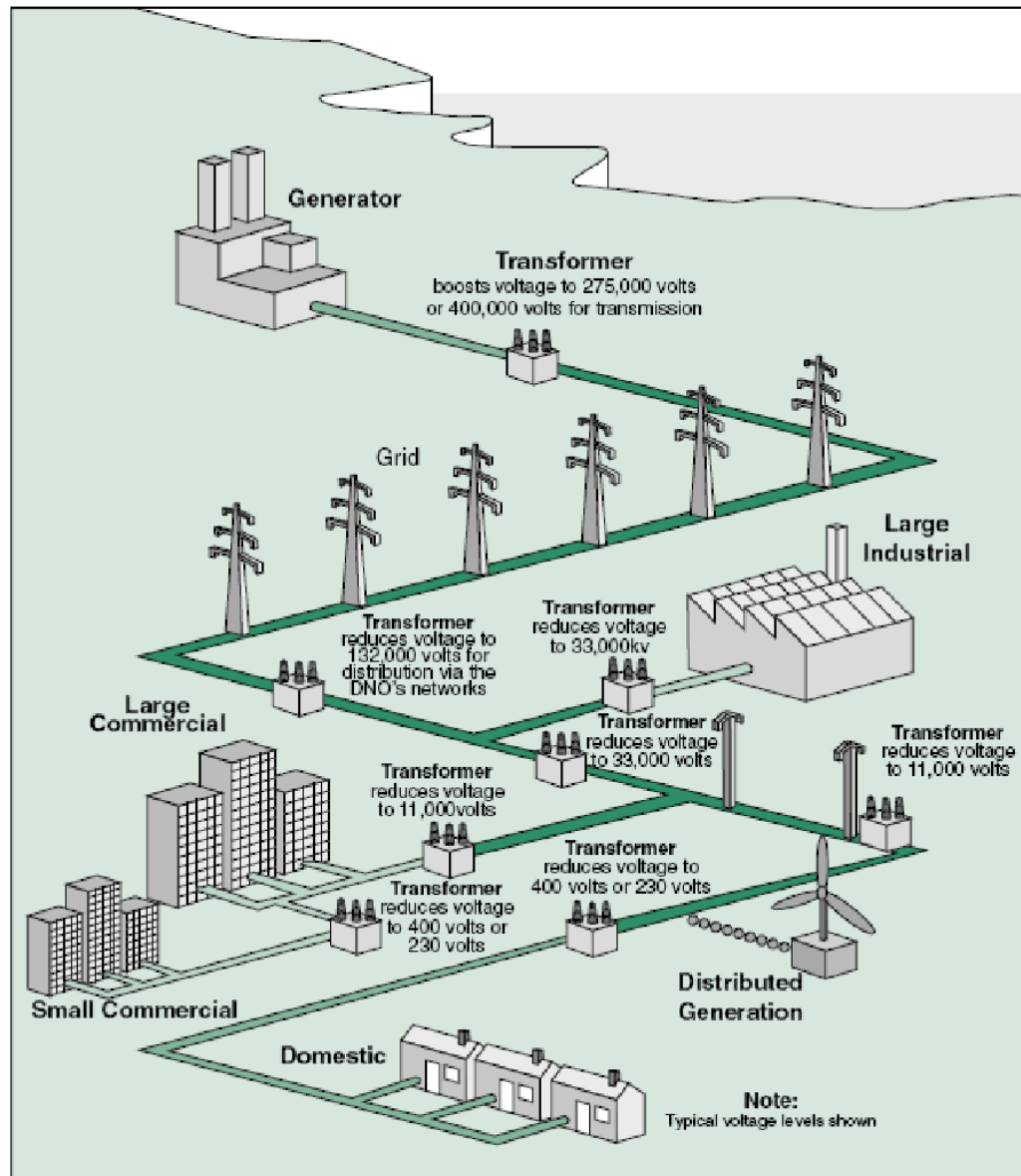


Figure 1.1: Simplified UK electrical power transmission system [1]

In an electricity network, some of the high voltage applications make use of sulphur hexafluoride (SF_6) gas as an insulation medium, such as in the gas insulated transmission line (GIL), gas insulated switchgear (GIS), and gas circuit breaker (GCB). Due to its superior insulation properties, SF_6 has been the primary insulator for many high end electrical applications. However, many studies show that SF_6 greenhouse effects raise concerns to its environmental impact. There are three major types of global

warming potential (GWP) gases: these are hydrofluorocarbons (HFCs), perfluorocarbons (PFCs), and SF₆. In addition to having high GWPs, SF₆ and PFCs have an extremely long atmospheric lifetime, resulting in an accumulation in the atmosphere once released [2]. Some of the studies in the awareness of the hazard caused by SF₆ have been well described in the following statements:

“SF₆ is a strong greenhouse gas and the molecule is very resistant against attack in the atmosphere. The natural self cleansing property of the atmosphere is insufficient to deal with such super molecules. Its production is now restricted under the Kyoto Protocol.” [3]

“Sulfur hexafluoride is the most potent greenhouse gas in existence. With a global warming potential 23,900 times greater than carbon dioxide, one pound of SF₆ has the same global warming impact of 11 tons of carbon dioxide.” [4]

“The atmospheric lifetime of SF₆ is 3,200 years, which results in essentially irreversible heat trapping within the atmosphere.” [5]

Takuma et al [6] stated in a report that although emission of SF₆ is relatively small compared to CO₂, the global warming potential (GWP) is the highest of all available gases. For that reason, the electrical power industry has been working hard to find a replacement for SF₆ with a smaller GWP and less environmental impact. In fact, Schneider Electric has introduced the Premset switchgear [7] and Mitsubishi Electric has introduced the Dry Air Insulated Switchgear [8] to be used in medium voltage distribution which are free from SF₆.

Until recently, researchers have been trying to find suitable alternatives for SF₆. Gases and gas mixtures, especially the ones containing carbon (C) and fluorine (F), can have better dielectric strength than SF₆. Some perfluorocarbons and related mixtures are showing breakdown strengths as high as 2.5 times that of SF₆, but these are also

greenhouse gases [9]. One of the very promising candidates is trifluoroiodomethane (CF_3I). Due to its high boiling point property, CF_3I gas is mixed with other gases such as CO_2 and N_2 to provide a more practical way of deploying it as an insulation medium, since CO_2 and N_2 have lower boiling temperatures.

1.2 Direction of Research and Objectives

The focus of this study is to provide a fundamental knowledge on the breakdown properties of CF_3I and its mixtures under lightning impulses. As mentioned earlier, it is fairly important to search for good prospective insulation gases in order to find an alternative for SF_6 . U_{50} and $V-t$ characteristics properties will offer an insight into how well the CF_3I gas mixtures behave as an insulation medium.

For the tests to be carried out successfully, a reliable experimental setup needs to be developed. This consisted of an air-tight pressure vessel, with all the security measures, fittings, and assemblies fitted, as well as generation and measurement of the lightning impulse, and the data acquisition of the test results. A reliable gap length control is particularly important. The entire available electrodes configuration should not disturb the gas mixtures inside the vessel.

A simulation technique is needed to determine the electrical field for any given test condition. This will ensure a full understanding of the level of the maximum electric field that the CF_3I gas mixtures can handle, and to provide better insight into actual performance under electric field behaviour. The specific objectives of this study are outlined below:

- i. To review current knowledge and trends in research interests related to this study, which include alternative gases for SF_6 , determination of the

electric field effects, factors affecting breakdown of gases, and measurement techniques in high voltage testing;

- ii. To build a novel pressure vessel as part of the test rig design and construction, with consideration given on the size, gas recovery system, gap control system, safety measures, and reliability of the vessel;
- iii. To investigate the breakdown properties of $\text{CF}_3\text{I-CO}_2$ mixtures under lightning impulse and several factors, such as electrode configurations, polarity of lightning impulse, gap length between electrodes, pressures and CF_3I content. The gap length is limited to 5cm while the maximum lightning impulse that can be applied is limited to around 170 kV in order to protect the HV bushing of the pressure vessel; and
- iv. To examine the electric field for each given test condition using an adequate model in simulation software.

1.3 Contribution of Thesis

The following contributions were achieved during this research programme:

- i. Extensive literature search on CF_3I properties and its potential for high voltage applications.
- ii. Designed and constructed a pressurised test chamber equipped with measurement and control apparatus, including CF_3I gas recycling.
- iii. Conducted extensive tests and collected data on CF_3I gas and its mixtures which allows better understanding of breakdown properties and dielectric strength.
- iv. Uniform and non-uniform field properties of the CF_3I gas and its mixtures were clarified and the effect of CF_3I content was quantified

- v. Microscopic analysis of breakdown by-products was achieved.

1.4 Organization of Thesis

This thesis is divided into seven chapters:

CHAPTER 2 provides an extensive review of published literature with regard to the study undertaken. A general overview of CF₃I gas and its mixtures are presented along with previous investigations by other researchers for numerous possible mixtures, such as CF₃I-air, CF₃I-N₂, and CF₃I-CO₂, with comparison to SF₆.

CHAPTER 3 presents the development of the test rig design and construction. A detailed explanation of the construction of the pressure vessel is presented. It includes all the considerations related to fittings and assemblies, such as material, pressure relief valve, gauges, linear actuator, and other equipment. This chapter aims to give an overview of the constructed gas evacuation and filling systems as well as how the system is being assembled and operated for mixing gases.

CHAPTER 4 reports investigation and calibration tests and results related to air breakdown. Some fundamental tests with air have been carried out to verify that the test rig is working properly and as means of calibration so that it can be used for further tests with CF₃I gas mixtures. Tests were carried out according to available standards, to determine the U₅₀ and *V-t* characteristics for different pressures. This chapter also presents the simulation studies undertaken with detailed explanation on the modelling to be used in numerical simulations.

CHAPTER 5 investigates the breakdown properties of CF₃I mixtures under lightning impulses. In this chapter, focus is given to CF₃I-CO₂ mixtures with a ratio of 30%-70%. Tests were carried out to investigate the effects of three electrode configurations, which are rod-plane, plane-plane, and sphere gap. The CF₃I-CO₂

mixture was subjected to both positive and negative lightning impulses. Also, the effect of gap length was investigated. Based on U_{50} results for a given test parameter, the electric field curves were determined to clarify the effect of electric field on breakdown of the gas.

CHAPTER 6, on the other hand, investigates the breakdown properties of CF_3I - CO_2 mixtures under lightning impulses for different ratios of CF_3I content apart from 30%-70%; these include 40%-60% and 20%-80%. These results will offer insight on how much influence the CF_3I gas has in terms of dielectric strength if it is mixed with CO_2 . In addition, the effect of pressure was investigated. CF_3I - CO_2 mixture with a ratio of 30%-70% was tested for up to 2 bars in a rod-plane gap with variable lengths.

CHAPTER 7 presents overall conclusions based on results and findings in this study and outlines recommendations for future investigations.

CHAPTER 2: CF₃I MIXTURES AS SF₆ ALTERNATIVE: A REVIEW

2.1 *Introduction*

Recent developments in the search for alternative gases to replace SF₆ gas throughout the electrical power industry have triggered numerous investigations on SF₆ mixtures, other gases, and mixtures of gases. This is in terms of fundamental characteristics of insulation such as breakdown strength, voltage-time ($V-t$) characteristics, partial discharge properties, fault interruption capability and others. Although many experimental works and tests have been carried out and presented by researchers [10], [11], [12], [13], [14], [15], there are still gaps that needed to be filled in order to convince the working committee to make a decision to replace SF₆ in high voltage applications.

The aim of this chapter is to provide a comprehensive review of the studies related to the research programme in order to provide a good understanding of one of the prospective gases in replacing SF₆ gas as an insulation medium. These include several factors including insulation characteristics, environmental properties, types of gas mixtures, and overall stability. A good understanding of these factors is vital in determining the implications and the protective performance of the gas mixtures.

2.2 *Sulphur Hexafluoride (SF₆) as an Insulation Gas*

Air is known as a preferred gas insulating medium in the electrical power system, but for more specific applications, such as gas insulated substations and circuit

breakers, sulphur hexafluoride (SF_6) has been widely used. SF_6 is regarded as the best gas insulation medium known in high voltage applications [6]. As indicated in the previous chapter, SF_6 is a greenhouse gas and many investigations have been carried out to find an adequate replacement [16].

Although SF_6 is colourless, odourless, and tasteless, its weight is approximately five times heavier than air. Since SF_6 is heavier than air, it tends to pool in low places, so there is a danger of suffocation through oxygen displacement. If the oxygen content in air is reduced to less than 13 percent from the normal 20 percent, nausea and drowsiness can occur [17].

When electrical discharges occur in equipment filled with SF_6 , toxic by-products can be produced. These by-products are a threat to the health of workers that come in contact with the by-products. There are four types of electric discharges which will lead to decomposition of SF_6 [18]:

- i. partial corona discharges,
- ii. spark discharges,
- iii. switching arcs, and
- iv. failure arcs.

SF_6 by-products, for examples gases such as hydrogen fluoride (HF), sulfur dioxide (SO_2), silicon tetrafluoride (SiF_4) and sulphur dioxide (SO_2), are very irritating to the eyes, nose, and throat [19]. James et. al. [20] reported that two workers collapsed after entering an SF_6 storage tower. One of the workers suffered pulmonary edema (excess collection of water fluid in the lungs) for three days. SF_6 and SO_2 were then detected at the area and both exceeded the threshold limit value (TLV).

CF_3I , on the other hand, has been used in fire extinguishing systems [21]. Just as SF_6 , CF_3I is also colourless, odourless, and electrically a non-conductive gas. In 1994,

Moore et. al. [22] prepared a report to illustrate the conclusion of several studies in order to replace Halon with CF_3I as a fire extinguisher. The report was based on a wide number of publications that focused on the following areas:

- i. fire suppression characteristics,
- ii. global environmental characteristics,
- iii. toxicology information,
- iv. stability for temperatures below 116 °C in the absence of light, oxygen, and water, and
- v. compatibility with other materials

It is reported that based on the toxicological, environmental, and fire fighting results for unoccupied areas and streaming applications, CF_3I was selected as a very good candidate to be used as Halon replacement, and this includes Halon 1301 and Halon 1211.

2.3 *Properties Required for Power System Applications*

In this section, several general characteristics for SF_6 replacement are provided for circuit breakers, gas-insulated transmission lines, and power transformers [23].

2.3.1 Circuit breaker applications

The most important physical characteristics of an insulating gas in circuit breakers (CBs) are related to the electric arc. The characteristics required for arc interruption are high dielectric strength, high interruption capability, which consist of high thermal conductivity and high electron attachment, quick gas recovery and the ability to re-form (self-healing).

2.3.2 Gas-insulated transmission lines (GIL) applications

The properties required for gas-insulated transmission line applications are different from the applications in circuit breakers. Important properties that the adopted gas needs to fulfil are high dielectric strength, long term stability, inertness and good thermal conductivity.

In particular, the gas needs to show a high dielectric strength under different stress conditions, such as uniform and non-uniform fields, electrode roughness and possible presence of conducting particles, and various geometric configurations. Although SF₆ is a good gas dielectric, its stability in non-uniform field is not as good as in uniform field, and this is a major issue [24].

There should be no possibility of chemical reaction within the electrode materials or the metallic structure and the sealing-materials in long-term use (40 years or more). There should also be no contaminations due to deposits, such as carbon deposits, polymerization, or decomposition. Other important characteristics connected to maintenance include being easily removable, having non-harmful by-products, and creating no hazards for personnel or structure, including no risk of fire, explosion, toxicity or corrosion.

2.3.3 Gas-insulated transformers applications

High rating power transformers use oils as dielectric and cooling media. However, several problems in the use of oil exist. The risk of ignition in the presence of air, breakdown due to contamination particles, and ion accumulation are all possible in insulation oils. The adoption of a gas instead of an oil can offer several advantages, such as lower risk of ignition and explosion, reduced weight of the machine and reduced noise overall (gas transmits less vibration than oil).

The properties that a gas should offer to be used successfully in power transformers are high dielectric strength at high pressure (e.g. 500 kPa), low toxicity, inertness, good thermal stability, no risk of fire, fire suppressor, high cooling capability, no reaction with various solid materials, good partial discharge characteristic, wide operative temperature range, easy to handle, a large amount available on the market and low price. Another important property is low boiling point, so that the gas will not liquefy at low temperature conditions, such as during winter time.

2.4 Physical and Chemical Properties of CF_3I

CF_3I is found to have attractive insulation properties. It is known with various names in industry. The most common synonyms for trifluoroiodomethane (CF_3I) include [25]:

- Iodotrifluoromethane,
- Trifluoromethyl Iodide, and
- Perfluoromethyl iodide.

The 3D molecular drawing for CF_3I is shown in Figure 2.1.

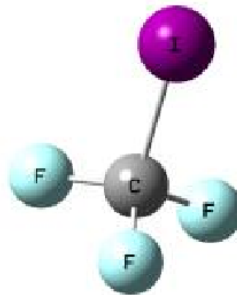


Figure 2.1: 3D molecular drawing of CF_3I , showing three fluorine atoms (light blue) and an iodine atom (purple) connected to a carbon atom (grey) [26]

CF₃I can be identified in the international databases using the following numbers:

- Chemical Abstracts Service (CAS) Number 2134-97-8 or
- European Chemical (EC) Number 219-014-5

Table 2.1 shows the physical properties of CF₃I.

Table 2.1: Physical properties of CF₃I [27]

Physical or Chemistry Property	Value or Description
Molecular weight	195.1
Physical state at 20°C	Gas
Melting point	- 110°C (- 166°F)
Boiling point at 1 atm	- 22.5°C (- 8.5°F)
Liquid density at - 32.5°C	2.36 g/mL
Odour threshold	Odourless
Solubility in water	Slight
Vapour pressure at 25°C	78.4 psia
Pressure-temperature curve	log psia = 5.7411-1146.82/T/K
Critical pressure	586 psia (estimated)
Critical temperature	122°C (estimated)
Critical volume	225 cm ³ /mole (estimated)
Electron affinity	150 ± 20 kJ/mole
Vapour heat capacity	16.9 cal/mole-K
C-I bond dissociation energy	54 kcal/mole
Vapour density (air = 1)	6.9

As discussed in Chapter 1 (*Introduction*), one of the main reasons for researchers to search for an alternative gas to replace SF₆ is due to the concern about the SF₆ greenhouse effects. The global warming potential (GWP) of SF₆ is so high that its production has been restricted under Kyoto Protocol [28]. CF₃I, on the other hand, has a

very low GWP. Table 2.2 below shows a comparison between CO₂, SF₆, and CF₃I in terms of environmental attributes.

Table 2.2: Lifetimes, radiative efficiencies and direct GWPs relative to CO₂ [29]

Gas	Life time (years)	Radiative efficiency (W m ⁻² ppb ⁻¹)	GWP for given time horizon (years)		
			20	100	500
CO ₂	N/A	1.4×10 ⁻⁵	1	1	1
SF ₆	3200	0.52	16300	22800	32600
CF ₃ I	0.005	0.23	1	0.4	0.1

In order to replace SF₆ with CF₃I successfully several physical characteristics need to be investigated. The first property that must be fulfilled is that of a high dielectric strength. The dielectric strength of the selected gas needs to offer a higher value than air and the same order of SF₆ in order to use the same design applied in current GIS systems. A comparative list with dielectric strength of various gases expressed as relative value to SF₆ is shown in Table 2.3:

Table 2.3: Breakdown strengths of selected gases relative to SF₆ [23], [30]

Gas	Relative strength to SF ₆	Electron attaching
C-C ₆ F ₁₂	≈2.4	Very strong or strong
C ₄ F ₆	≈2.3	
C-C ₄ F ₆	≈1.7	
C-C ₄ F ₈	1.3	
CF ₃ I	1.21 (107.7 kV/cm)	
SF ₆	1.0 (89 kV/cm)	
C ₃ F ₈	0.9	Weak
CO	0.4	
N ₂ O	0.44	
CO ₂	0.3	
Air	≈0.3	
N ₂	0.36	Non-attaching
H ₂	0.18	

2.4.1 Electron Interaction Properties

It has been reported in [23] that in order to present good dielectric strength, the gas should present with the ability to reduce the number of free electrons. Therefore the following properties need to be considered:

- electron attachment or electronegative property for removing free electrons by attachment;
- the ionization cross section should present a low value in order to offer a reduced number of free electrons;
- electron slowing-down properties should allow a slowdown of electrons in order to facilitate their capture at lower energy; and
- the electron impact ionization should have a high value as it prevents the ionization by electron impact.

De Urquijo et al. [31], [32], [33] as well as Deng and Xiao [34] have determined electron interaction properties of CF_3I , $\text{CF}_3\text{I-N}_2$ and $\text{CF}_3\text{I-CO}_2$ mixtures using a pulse Townsend experiment and Boltzmann equation analysis. In particular, the electron drift velocity v_e , the effective ionization coefficient $(\alpha-\eta)/N$, and the limiting field strength E/N_{lim} for CF_3I and its mixture with N_2 and CO_2 at different percentages were published. In these properties, α is electron impact ionization coefficient, η is the attachment coefficient, E is the electric field and N is the gas density.

2.4.1.1 Electron Drift Velocity, v_e

Figure 2.2 depicts the electron drift velocities for $\text{CF}_3\text{I-N}_2$ and $\text{CF}_3\text{I-CO}_2$ for various levels of pressure in comparison with SF_6 .

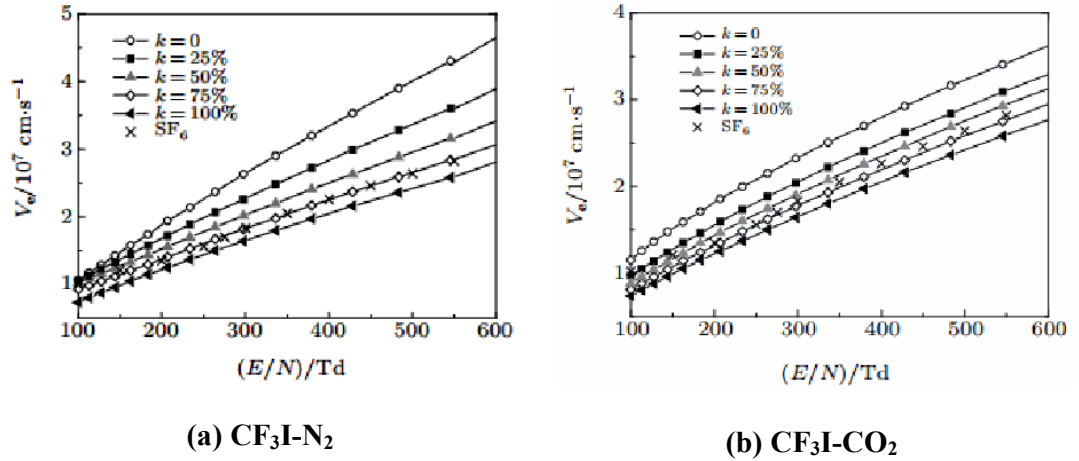


Figure 2.2: Electron drift velocities as a function of E/N at different CF₃I ratio k in comparison with SF₆ [34]

It is clear that the electron drift velocity (v_e) decreases as the CF₃I content increases for both gas mixtures, as expected with an electronegative gas as in CF₃I. The v_e for CF₃I-N₂ mixtures of 75%-25% gives the same value with those of SF₆. Using the same mixture ratio, CF₃I-CO₂ gives slightly lower v_e than SF₆.

2.4.1.2 Effective Ionization Coefficient, $(\alpha-\eta)/N$

The density-normalized effective ionization coefficient $(\alpha-\eta)/N$, calculated by Deng and Xiao [34], indicates that $(\alpha-\eta)/N$ increases when E/N increases for both CF₃I-N₂ and CF₃I-CO₂ gas mixtures, as shown in Figure 2.3. Interestingly, for CF₃I-N₂ mixtures, where E/N is more than 300 Td, the increment of $(\alpha-\eta)/N$ for the mixtures tends to be higher than that of pure N₂ itself. This calculation has been confirmed by de Urquijo et al. [31] as noted in the experimental results.

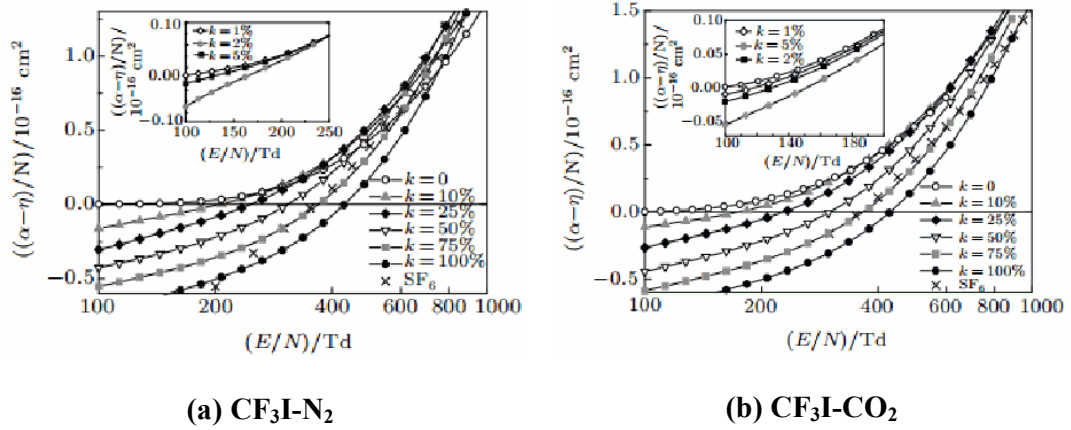


Figure 2.3: Density-normalized effective ionization coefficients $(\alpha-\eta)/N$ as a function of E/N at different CF_3I gas mixture ratio k in comparison with SF_6 [34]

2.4.1.3 Limiting field strength, E/N_{lim}

The limiting field strength, E/N_{lim} is given when ionisation is equal to attachment, $\alpha = \eta$ and when $(\alpha-\eta)/N = 0$. The critical field strength of pure CF_3I is 473 Td, and is higher than that SF_6 which is 361 Td [31], [32], [33]. Figure 2.4 depicts the E/N_{lim} values for CF_3I-N_2 and CF_3I-CO_2 mixtures in comparison with SF_6-N_2 mixture, since it has been widely used as a binary gas mixture for power equipment [34].

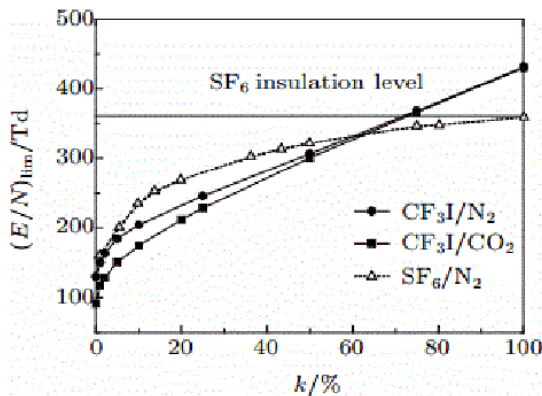


Figure 2.4: The limiting field, E/N_{lim} as a function of CF_3I and SF_6 gas content k [34]

For a lower content of CF₃I (< 30%) in its mixtures, E/N_{lim} of CF₃I-N₂ is higher than that of CF₃I-CO₂. In mixtures where CF₃I is more dominant, the E/N_{lim} values are the same for both mixtures, and at 60% or more of CF₃I, the E/N_{lim} values are higher than SF₆-N₂. If the content of CF₃I is more than 75%, mixtures of CF₃I with N₂ or CO₂ are even better for pure SF₆.

2.5 Thermal Properties of CF₃I

A good gas insulation medium for high voltage equipment should show good characteristics under high vapour pressure and high temperature. A high vapour pressure avoids the possibility of phase change from gas into liquid for a given temperature range. High thermal conductivity, on the other hand, ensures the gas has a good cooling characteristic. In this part, saturation vapour pressure curve for CF₃I is analyzed.

Duan et al. [35] measured the saturated densities of the gas from which the critical point parameters were calculated:

- critical density ρ_c 868 kg m⁻³
- critical temperature T_c 396.44 K (123 °C)
- critical pressure P_c 3.953 MPa

In another study, Duan et al. [36] measured several vapour pressure data points for CF₃I and an analytical correlation of pressure and densities were derived. The pressure-temperature conditions of phase change are demonstrated by:

$$\ln\left(\frac{P}{P_c}\right) = (A_1\tau + A_2\tau^{1.25} + A_3\tau^3 + A_4\tau^7) \frac{T_c}{T} \quad (2.1)$$

where

$$\tau: \quad 1-T/T_c$$

- T_c : critical temperature
- P_c : critical pressure
- A_i : coefficients, as shown in Table 2.4

Table 2.4: Coefficients for Eqn. (2.1) [36]

A_1	A_2	A_3	A_4
-7.19045	1.34829	-1.58035	-5.46680

The saturation vapour pressure curve for CF_3I is then plotted using MATLAB based on Eqn. (2.1). Figure 2.5 below, shows the CF_3I curve along with those for SF_6 , CO_2 , and N_2 , which are taken from [37], [38], and [39]. Figure 2.6 shows the same curves for pressure between 0.1 MPa to 1.0 MPa.

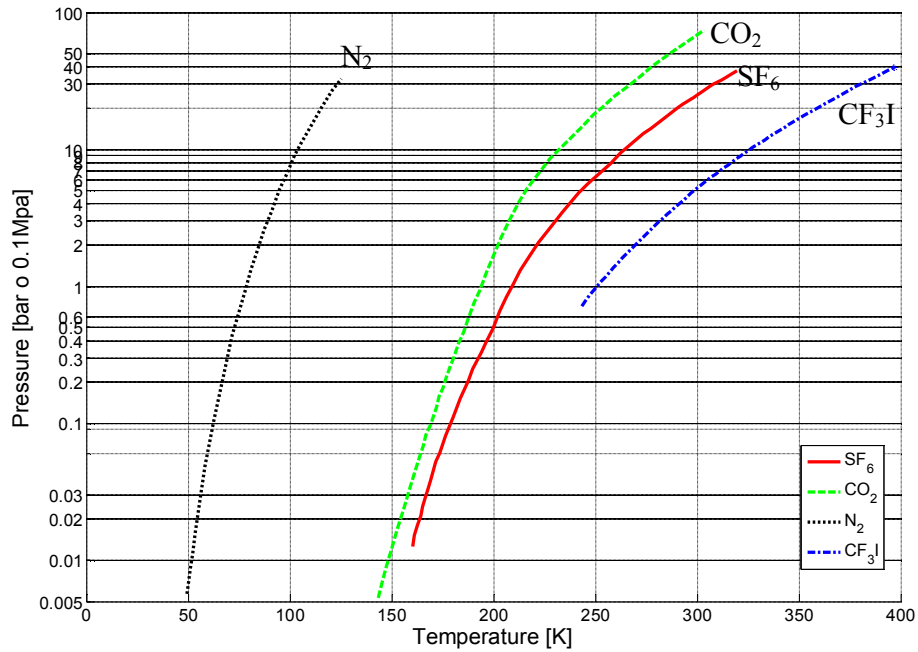


Figure 2.5: Saturation vapour pressure curves for SF_6 , CO_2 , N_2 , and CF_3I

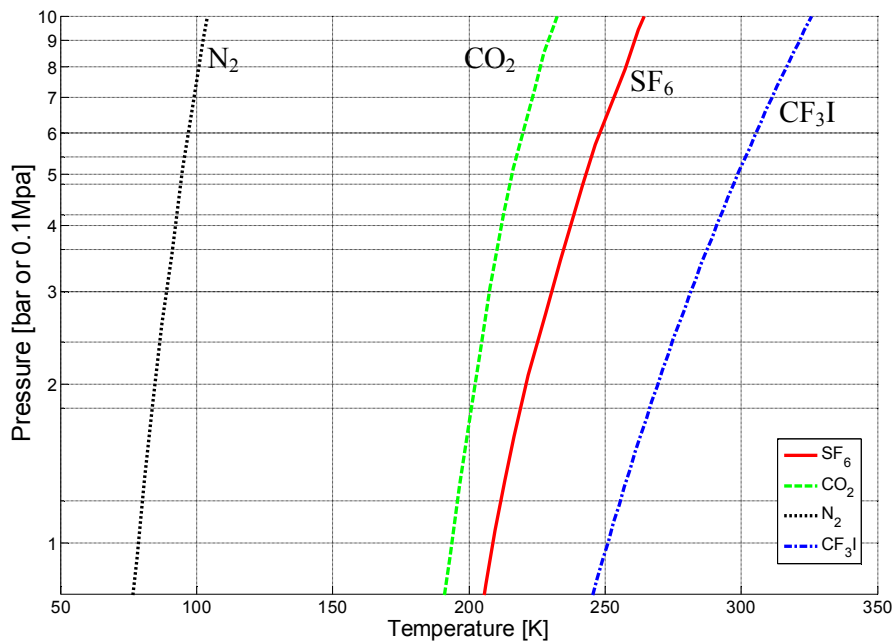


Figure 2.6: Saturation vapour pressure curves for SF₆, CO₂, N₂, and CF₃I (0.1 MPa to 1.0 MPa)

Based on Figure 2.6, at 0.1 MPa, the boiling points for CF₃I and SF₆ are approximately 251K (–22.15°C) and 208K (–65.15°C), respectively. According to Katagiri et al. [40], a typical gas-insulated circuit breaker (GCB) for GIS uses SF₆ gas at 0.5 MPa as the insulation medium. Again, by referring to Figure 2.6, at 0.5 MPa, the boiling points for CF₃I and SF₆ are given at around 298 K (24.85°C) and 243 K (–30.15°C). As a reference, Figure 2.7 shows the saturation vapour pressure curves for CF₃I and SF₆ as given by Katagiri in [40].

It is clear that it can be difficult to use compressed pure CF₃I in HV switchgear under these conditions. As an example, during winter times in certain countries, the temperature may drop to lower than –22.15°C. If this occurs, then the CF₃I gas will liquefy. The adoption of other gases, such as nitrogen (N₂) or carbon dioxide (CO₂) as a

mixture in CF_3I , helps in reducing the boiling point, and it is absolutely required for outdoor application. This is required in order to prevent CF_3I from liquefying.

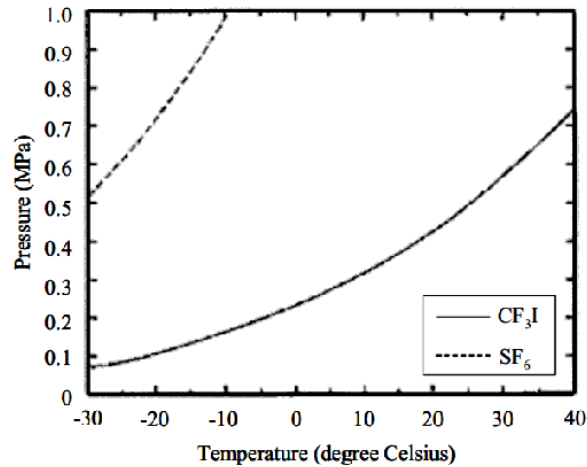


Figure 2.7: Saturation vapour pressure curves for CF_3I and SF_6 as given by [40]

According to Dalton's law, the total pressure of mixture of gases equals the sum of the pressures that each would exert if it were present alone as depicted in Eqn. (2.2) below.

$$P_T = P_1 + P_2 + \dots + P_n \quad \text{or} \quad P_T = \sum_{i=1}^n P_i \quad (2.2)$$

where

P_1, P_2, \dots, P_n represent the partial pressure of each gas

Kasuya et al. [41], [42] and Katagiri et al. [40], [43] reported that at 0.5 MPa, the boiling point of $\text{CF}_3\text{I}-\text{CO}_2$ (40%-60%) and $\text{CF}_3\text{I}-\text{CO}_2$ (30%-70%) gas mixtures are about -5°C and -12°C , respectively. Referring to Figure 2.6, the boiling point for pure CF_3I gas at 0.5 MPa is around 300 K (26.85°C). Further discussion on the boiling point of $\text{CF}_3\text{I}-\text{CO}_2$ gas mixtures is presented in Section 6.3.3.

2.6 Electrical Properties of CF₃I and Its Mixtures

Insulation properties, such as voltage-time ($V-t$) characteristics, 50% breakdown voltage (U_{50}), and interruption capabilities, need to be investigated before a gas or gas mixture is used as a gas insulation medium in high voltage applications. Many researchers are focusing on mixing CF₃I with either CO₂ or N₂, since both gases are easily available and have a much lower boiling point [40], [44], [41]. However, due to the fact that CF₃I has just recently become known (less than 20 years) to have promising insulation characteristics, investigation reports on CF₃I and its mixtures are not as many as for SF₆. Only recently has there been progressive work on CF₃I mixtures. Hence the opportunity to explore its capabilities as an insulation medium is expansive.

2.6.1 50% Breakdown Voltage (U_{50})

It is possible to investigate U_{50} as a self-restoring insulation, such as a gas insulator, and in this case, CF₃I. U_{50} can be evaluated by using two methods [45]:

- i. the multiple-level method with at least four (4) voltage levels, and at least ten (10) impulses per level, and
- ii. the up-and-down method with one (1) impulse per group and at least twenty (20) useful applications.

2.6.1.1 50% Breakdown Voltage (U_{50}) of CF₃I

It is known that CF₃I has a dielectric strength of around 1.21 times higher than SF₆ [23], [30]. Toyota et al. [46] evaluated U_{50} for both SF₆ and CF₃I gases in their research. Under the application of a steep front square voltage with a wave front of 16 ns, Toyota measured the U_{50} using the up-and-down method, and the results are shown

in Table 2.5. The measurements were carried out with a rod-plane gap, with the tip radius of the electrode is given as 0.4 mm, the pressure was 0.1 MPa.

Table 2.5: 50% breakdown voltage, U_{50} , for SF₆ and CF₃I gases at 0.1 MPa under steep front square voltage application [46]

Gas	Gap length	Polarity	U_{50}
SF ₆	10 mm	Positive	47 kV
		Negative	-52 kV
	20 mm	Positive	64 kV
		Negative	-98 kV
CF ₃ I	10 mm	Positive	35 kV
		Negative	-61 kV
	20 mm	Positive	46 kV
		Negative	-84 kV

From the above table, for a gap length of 10 mm, U_{50} for CF₃I is around 0.74 times lower than SF₆ under positive polarity, but 1.17 times higher than SF₆ under negative polarity. Meanwhile, for a gap length of 20 mm, in both polarities, U_{50} for CF₃I is lower than SF₆, with 0.72 times under positive polarity and 0.86 times under negative polarity.

However, there is inconsistency within the negative polarity results. For a 10 mm gap length, U_{50} for CF₃I is lower than SF₆, while it is higher in a 20 mm gap length. This is due to a change in the gap geometry, and hence, a change in field utilization factor. For a rod-plane electrode system, an increase in gap length will result in a decrease in field utilization factor, which represents more non-uniform electric field configuration. As have been reported by Takeda et al. [47], CF₃I has lower sparkover voltages in lower field utilization factors, as compared to SF₆.

2.6.1.2 50% Breakdown Voltage (U_{50}) of CF_3I Mixtures

Further tests on U_{50} have been carried out by Katagiri et al. [40]. For these measurements, CF_3I was mixed with CO_2 in various ratios to investigate the effects of CF_3I content on a given test condition. By applying standard lightning impulse voltage, with a sphere gap of 10 mm apart, the results on the aforementioned tests were obtained (see Figure 2.8).

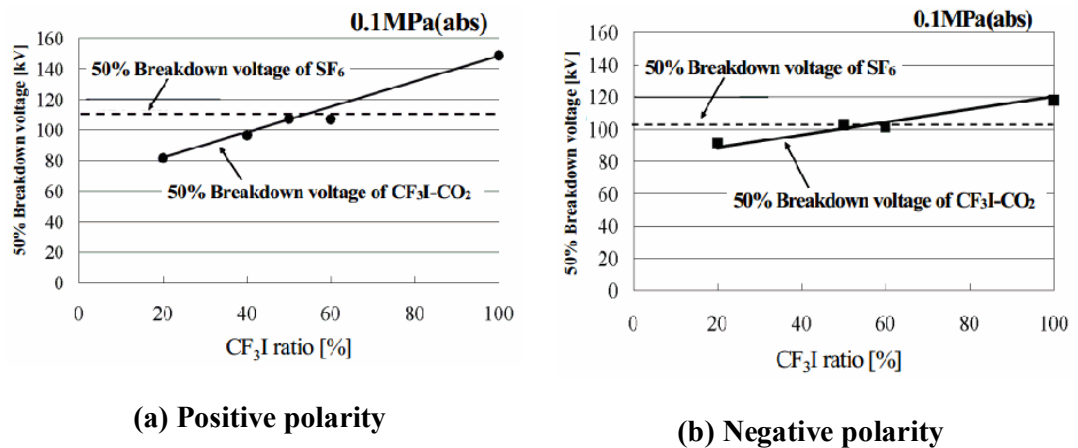


Figure 2.8: U_{50} for CF_3I - CO_2 mixtures [40]

For this electrode system, it is clear that the U_{50} for pure CF_3I is higher than the given U_{50} of SF_6 , which is around 1.2 times better. In both polarities, the U_{50} curves increase linearly with the proportion of CF_3I . At a CF_3I ratio of 60%, the dielectric strength of the CF_3I - CO_2 mixture is close to that of SF_6 . The U_{50} for SF_6 presented is higher than the rated 89 kV, due to the tests being carried out with lightning impulse, where statistical effect of electron production plays a major role. According to Anis and Srivastava [48], the space charge due to corona under lightning impulses does not have sufficient time to stabilize, which is also related to rate of production of initiatory electrons. A lightning impulse, which happens in a very short period, then requires higher electric field (and hence higher voltage) to provide a condition for breakdown.

Under static electric field conditions, such as in dc voltage, the U_{50} for SF_6 would be around 89 kV.

However, according to Katagiri et al., because of the high boiling point of CF_3I , the proportion of CF_3I in the mixture should not be more than 30% which gives the dielectric strength of CF_3I-CO_2 (30%-70%) of around 0.75 to 0.8 times that of SF_6 . It should be noted that these measurements were carried out with only fifteen (15) breakdown tests [40]. If the measurements were using an up-and-down method, the tests should be carried out with at least twenty (20) useful applications to conform to the international standard BS EN 60060-1 (2010) [32].

2.6.2 V-t characteristics

Another characteristic used to evaluate the insulation performance for a gas, considers the $V-t$ characteristic which represents the relationship between the breakdown voltage and time to breakdown. If the voltage used in the measurements is a standard lightning impulse waveform, the breakdown can occur before, after, or at the peak value. The value of voltage when the breakdown occurs and its associated time lag are recorded and used to plot the $V-t$ characteristics, as shown in Figure 2.9.

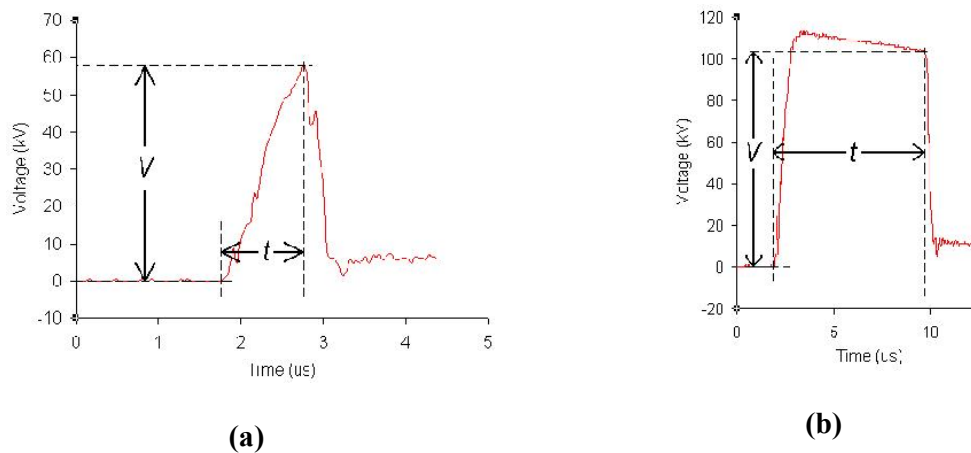


Figure 2.9: Breakdown (a) before and (b) after peak of lightning impulse

2.6.2.1 V-t characteristics of pure CF₃I

In 2005, Toyota et al. [46], [49] compared CF₃I V-t characteristics with SF₆, with emphasis given to non-uniform field conditions. Toyota applied a steep-front square voltage with a front wave of 16 ns and a peak value up to 200 kV. These short time range measurements are useful in dealing with very fast, transient overvoltage problems caused in GIS. Another impulse voltage has been used in the tests characterised as 1.8/450 μs, in which the wave front was similar to the lightning impulse.

The electrodes were configured as rod-plane system, with a radiation source installed behind the plane electrode to promote the initial electrons generation. By using Cobalt-60, the electrons are accelerated towards the anode. This irradiation technique was used to overcome the statistical variability [48]. The results are shown in Figure 2.10 and Figure 2.11.

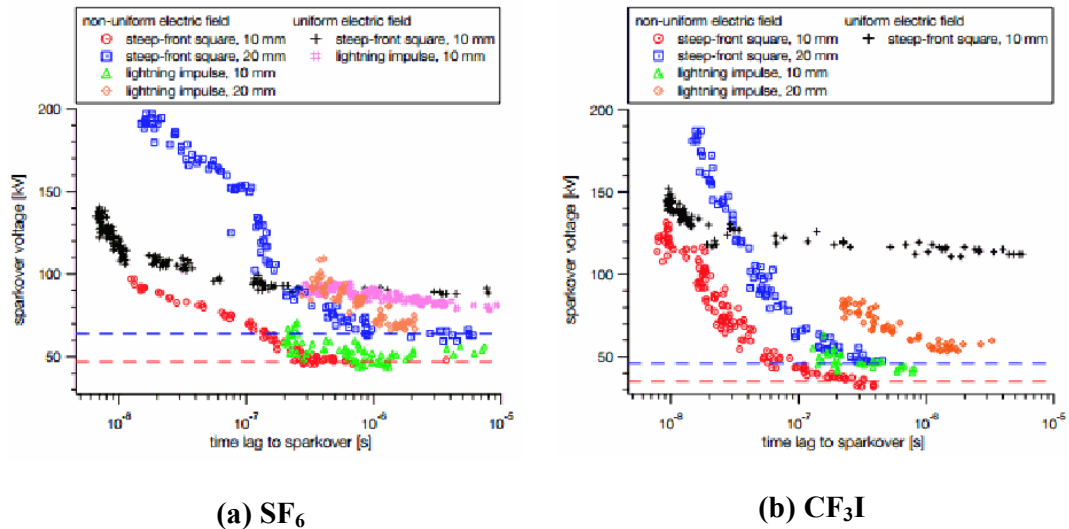


Figure 2.10: V-t characteristics at 0.1 MPa [46] under positive polarity. Dashed lines indicate U₅₀ in Table 2.5

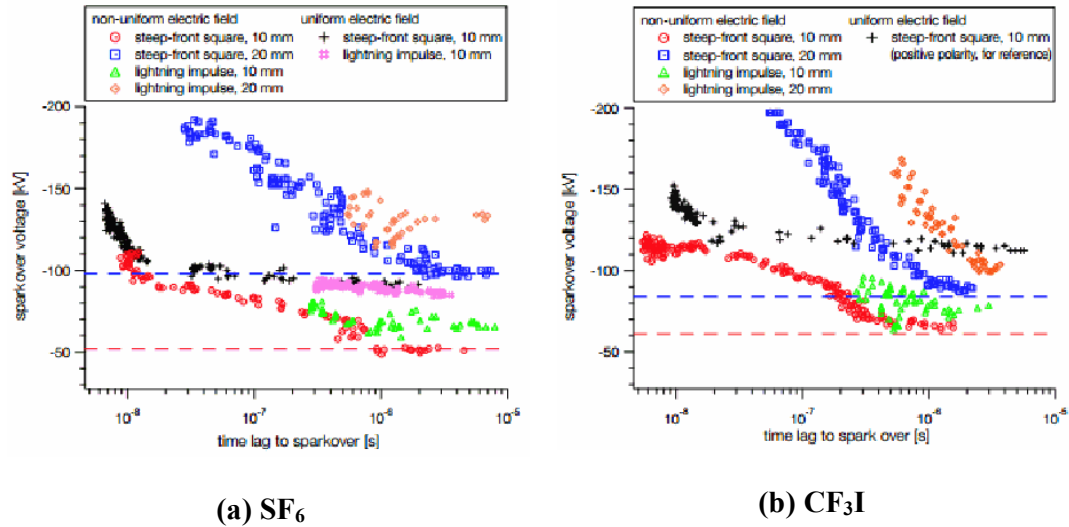


Figure 2.11: $V-t$ characteristics at 0.1 MPa [46] under negative polarity. Dashed lines indicate U_{50} in Table 2.5

Toyota found that for the same period, in the time lag (t), the sparkover voltage (V) under steep front square voltage is lower than those at 1.8/450 μ s lightning impulses (non-standard). This effect is not easily explained.

Takeda et al. [47], [50], [51] carried out further tests on $V-t$ characteristics for CF₃I with more options in electrode configurations, by applying the same steep front square voltage. The field utilization factor, which is a function of the geometrical characteristic (the mean electric field/the maximum electric field) for each electrode configuration are shown in Table 2.6. Takeda's findings are summarized in the Figure 2.12.

Figure 2.12 shows that higher field utilization factors (0.38 onwards) for CF₃I, have higher $V-t$ characteristics (the $V-t$ characteristics shifted upwards), while for a low field utilization factor, SF₆ is better in terms of $V-t$ characteristics. This might be of interest since in order for CF₃I to replace SF₆ fully as an insulation medium, CF₃I has to have a better $V-t$ characteristics for all types of electrode configurations, since they represent various kinds of high voltage apparatus.

Table 2.6: Field utilization factors for different electrode configurations [47]

Electrode configuration	Field utilization factors
100 mm hemisphere	0.89
ϕ 12 mm hemispherical rod	0.45
ϕ 6 mm hemispherical rod	0.38
Conical rod ($r=0.4$ mm)	0.095

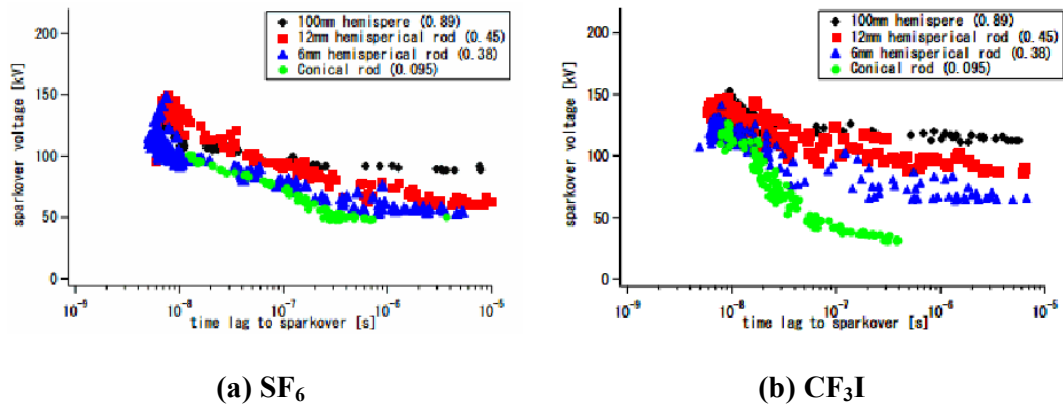


Figure 2.12: $V-t$ characteristics for gap 10mm; positive polarity [47]

2.6.2.2 $V-t$ Characteristics of CF_3I Mixtures

In 2006, Nakauchi et al. [52] reported that sparkover voltage in a CF_3I-N_2 mixture is almost the same as that in a CF_3I-CO_2 mixture under square pulse voltage. Toyota et al. [49] carried out further tests on $V-t$ characteristics for several CF_3I mixtures, namely CF_3I-N_2 and CF_3I-Air mixtures. A 50 mm radius hemisphere-to-plane electrode is used in the tests, giving a field utilization factor of 0.89 when the gap is 10 mm. Again, the CF_3I mixtures were subjected to steep front square wave voltage with a rise time of 20 ns. The total pressure of the gas is 0.1 MPa. The tests are carried out for positive polarity only. Figure 2.13 shows the summary of these findings [49].

It can be concluded that the $V-t$ characteristics for both CF_3I-N_2 mixtures are almost identical. For both mixtures, with a CF_3I ratio at 60%, the $V-t$ characteristics will

be the same as that of pure SF₆, as has also been reported in [53]. Therefore, the same dielectric strength is obtained. This is the same amount Katagiri et al. [40] reported in the investigation on U₅₀ for CF₃I-CO₂ mixtures, in which around 60% of CF₃I, the CF₃I-CO₂ mixture gives approximately the same voltage level as U₅₀ for SF₆.

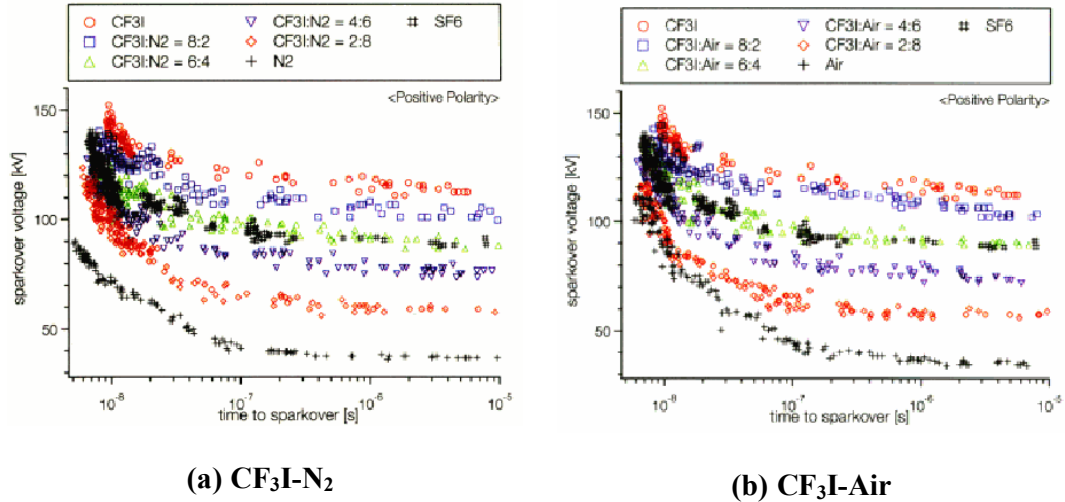


Figure 2.13: *V-t* characteristics at 0.1 MPa [49]

2.6.3 Other electrical properties for CF₃I and its mixtures

Interruption capabilities of CF₃I have been investigated by Katagiri et al. [40] and [54], Taki et al. [44] and Kasuya et al. [41]. Using a model of an arc-extinguishing chamber, the authors investigated short line fault (SLF) and breaker terminal fault (BTF) interruption capabilities of CF₃I, CF₃I-N₂, and CF₃I-CO₂ mixtures compared to SF₆. It was found that although dielectric strength of CF₃I is 1.2 times higher than SF₆, SLF interruption performance of CF₃I is around 0.9 times that of SF₆, and BTF interruption performance is almost 0.7 times that of SF₆.

Katagiri also reported that the interruption performance of CF₃I-CO₂ mixtures is higher than CF₃I-N₂ mixtures. This is thought to be due to the electron attaching

properties of CO_2 which are better than N_2 . A clearer view of this is depicted in Figure 2.14. An interesting point to be considered is that for $\text{CF}_3\text{I}-\text{CO}_2$ mixtures with at least 30% of CF_3I , interruption performance is almost the same of that of pure CF_3I . This gives a good indication, in terms of boiling point, of the gas mixture.

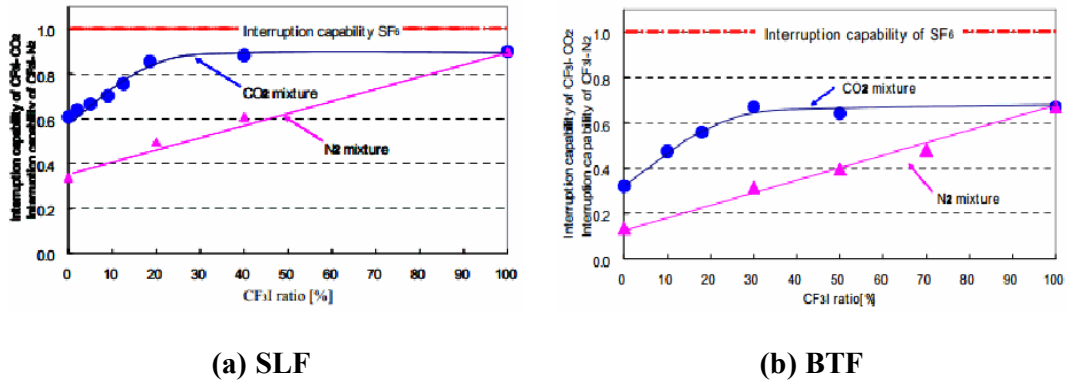


Figure 2.14: Interruption capabilities of CF_3I , $\text{CF}_3\text{I}-\text{N}_2$ and CF_3-CO_2 mixtures as compared to SF_6 [40]

Takeda et al. [47] and [55] carried out further tests on CF_3I to investigate surface flashover characteristics. A polytetrafluoroethylene (PTFE) dielectric is placed between two plane electrodes, immersed in CF_3I gas, with the application of steep front square wave voltage. It was found that, upon a surface discharge in CF_3I , the subsequent flashovers are lower than the previous ones. Upon investigation, a brownish material is found to be deposited on the PTFE surface, and this was later identified as iodine. The deposition of iodine increases with each flashover. It is possible that solid iodine deposited along the path of flashover may conduct current and, hence, may decrease the insulation performance of CF_3I gap.

2.7 By-products of CF_3I

One of the major concerns in SF_6 use is by-product production upon electrical discharges. SF_6 by-products, such as SO_2F_2 , SiF_4 , and SO_2 , are very irritating to the eyes, nose, and throat [19]. Due to this, the need to investigate the by-products of CF_3I , particularly in terms of insulation performance and dielectric strength are present.

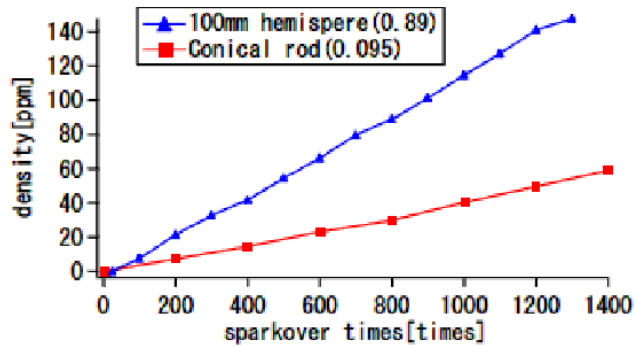


Figure 2.15: Relation between C_2F_6 and amount of sparkover times with different electrodes [57]

Investigations on gaseous decomposition of CF_3I have been carried out by Takeda et al. [47] and [57] and Kamarol et al. [58], using gas chromatography-mass spectrometry (GC-MS) to measure the by-products qualitatively and quantitatively. In the measurements, C_2F_6 , C_2F_4 , CHF_3 , C_3F_6 , C_3F_8 , and C_2F_5I are detected as gaseous by-products generated by sparkover. In these investigations, the amount of these by-products is found to be higher under uniform fields than that in non-uniform fields. This is due to the fact that higher breakdown voltage is needed in uniform fields, which related proportionally to the energy (energy, $E \propto V^2$) produced during the breakdown. C_2F_6 has the highest quantity among the gases, and this decomposition seems to be linearly increased in conjunction with amount of sparkover time, as depicted in Figure

REFERENCES

- [1] Commons Select Committees, “House of Commons - The Future of Britain’s Electricity Networks - Energy and Climate Change,” *Parliamentary*, 2010. [Online]. Available: <http://www.publications.parliament.uk/pa/cm200910/cmselect/cmenergy/194/19404.htm>. [Accessed: 30-Jul-2013].
- [2] United States Environmental Protection Agency (EPA), “SF₆ Emission Reduction Partnership for Electric Power Systems,” 2008. [Online]. Available: <http://www.epa.gov/electricpower-sf6/basic.html>.
- [3] Environmental News Service, “Potent New Greenhouse Gas Discovered,” 2000. [Online]. Available: <http://www.fluoridealert.org/news/potent-new-greenhouse-gas-discovered/>.
- [4] Environment News Service, “California Limits SF₆, World’s Most Potent Greenhouse Gas,” 2010. [Online]. Available: <http://www.ens-newswire.com/ens/mar2010/2010-03-02-091.html>.
- [5] J. Witkin, “California to Regulate ‘Most Potent’ Greenhouse Gas,” 2010. [Online]. Available: <http://green.blogs.nytimes.com/2010/03/10/california-to-regulate-most-potent-greenhouse-gas/>.
- [6] T. Takuma, O. Yamamoto, and S. Hamada, “Gases as a Dielectric,” in in *Gaseous Dielectrics X*, L. G. Christophorou, J. K. Olthoff, and P. Vassiliou, Eds. New York: Springer Science + Business Media, Inc., 2004, pp. 195–204.
- [7] Schneider Electric, “Innovation for MV distribution,” 2012.
- [8] Mitsubishi Electric, “Dry Air Inulated Switchgear,” 2013. [Online]. Available: <http://www.mitsubishielectric.com/company/environment/ecotopics/technologies/prod/switchgear/index.html>. [Accessed: 11-May-2013].
- [9] X. Q. Qiu, I. D. Chalmers, and P. Coventry, “A Study of Alternative Insulating Gases to SF₆,” *Journal of Physics D: Applied Sciences*, vol. 32, pp. 2918–2922, 1999.
- [10] Y. Qiu and E. Kuffel, “Comparison of SF₆/N₂ and SF₆/CO₂ Gas Mixtures as Alternatives to SF₆ Gas,” *IEEE Transactions on Dielectrics and Electrical Insulation*, vol. 6, no. 6, pp. 892–895, 1999.
- [11] Y. Qiu and Y. P. Feng, “Investigation of SF₆-N₂, SF₆-CO₂ and SF₆-Air as Substitutes for SF₆ Insulation,” in *IEEE International Symposium on Electrical Insulation*, 1996, no. 2, pp. 766–769.

- [12] M. Hikita, S. Ohtsuka, S. Okabe, and S. Kaneko, "Insulation Characteristics of Gas Mixtures including Perfluorocarbon Gas," *IEEE Transactions on Dielectrics and Electrical Insulation*, vol. 15, no. 4, pp. 1015–1022, 2008.
- [13] M. Hikita, S. Ohtsuka, S. Okabe, and G. Ueta, "Breakdown Mechanism in C₃F₈/CO₂ Gas Mixture under Non-Uniform Field on the Basis of Partial Discharge Properties," *IEEE Transactions on Dielectrics and Electrical Insulation*, vol. 16, no. 5, pp. 1413–1419, Oct. 2009.
- [14] N. Koshino, Y. Yoshitake, N. Hayakawa, and H. Okubo, "Partial Discharge and Breakdown Characteristics of CO₂-Based Gas Mixtures as SF₆ Substitutes," in in *Gaseous Dielectrics X*, L. G. Christophorou, J. K. Olthoff, and P. Vassiliou, Eds. New York: Springer Science + Business Media, Inc., 2004, pp. 217–222.
- [15] K. Mochizuki, T. Ueno, H. Mizoguchi, S. Yanabu, S. Yuasa, and S. Okabe, "Evaluation of Interruption Capability on Various Gases," in in *Gaseous Dielectrics X*, L. G. Christophorou, J. K. Olthoff, and P. Vassiliou, Eds. New York: Springer Science + Business Media, Inc., 2004, pp. 265–270.
- [16] H. Okubo and N. Hayakawa, "Dielectric Characteristics and Electrical Insulation Design Techniques of Gases and Gas Mixtures as Alternatives to SF₆," in in *Gaseous Dielectrics X*, L. G. Christophorou, J. K. Olthoff, and P. Vassiliou, Eds. New York: Springer Science + Business Media, Inc., 2004, pp. 243–252.
- [17] U.S. Environmental Protection Agency, "SF₆ Gas Handling Procedure."
- [18] ICF Consulting, "Byproducts of SF₆ Use in the Electric Power Industry," 2002.
- [19] U.S. National Library of Medicine, "Hazardous Substances Data Bank (HSDB)," 2011. [Online]. Available: <http://toxnet.nlm.nih.gov/cgi-bin/sis/htmlgen?HSDB>. [Accessed: 11-May-2013].
- [20] D. R. James, I. Sauers, G. D. Griffin, R. J. Van Brunt, J. K. Olthoff, K. L. Stricklett, Y. F. Chu, J. R. Robins, and H. D. Morrison, "Investigation of S₂F₁₀ Production and Mitigation in Compressed SF₆-insulated Power Systems," *IEEE Electrical Insulation Magazine*, vol. 9, no. 3, pp. 29–41, 1993.
- [21] The British Standard, "Gaseous Fire-Extinguishing Systems — Physical Properties and System Design," vol. 3. 2006.
- [22] T. A. Moore, S. R. Skaggs, M. R. Corbitt, R. E. Tapscott, D. S. Dierdorf, and C. J. Kibert, "The Development of CF₃I as a Halon Replacement," The University of New Mexico, 1994.
- [23] L. G. Christophorou, J. K. Olthoff, D. S. Green, U. S. G. P. Office, and E. D. and P. M. Division, "Gases for Electrical Insulation and Arc Interruption: Possible Present and Future Alternatives to pure SF₆," National Institute of Standards and Technology, 1997.

- [24] E. Onal, "Breakdown Characteristics of Gases in Non-Uniform Fields," *Journal of Electrical and Electronics Engineering - Istanbul University*, vol. 4, no. 2, pp. 1177–1182, 2004.
- [25] National Institute of Standards and Technology, "Methane, trifluoroiodo-," *NIST Reference Standard Data*, 2011. [Online]. Available: <http://webbook.nist.gov/cgi/cbook.cgi?Formula=cf3i&NoIon=on&Units=SI>. [Accessed: 14-May-2013].
- [26] Molecular Spectroscopy Group of Ca'Foscari University, "Molecules Investigated." [Online]. Available: <http://venus.unive.it/molspectragroup/Molecules/MoleculesBody.htm>. [Accessed: 13-May-2013].
- [27] Subcommittee on Iodotrifluoromethane, Committee on Toxicology, Board on Environmental Studies and Toxicology, and Division on Earth and Life Studies, *Iodotrifluoromethane: Toxicity Review*. Washington, D.C.: National Academic Press, 2004.
- [28] United Nations, "Kyoto Protocol to the United Nations Framework Convention on Climate Change," 1998.
- [29] IPCC Core Writing Team, R. K. Pachauri, and A. Reisinger, "Addendum-Errata of Climate Change 2007 Synthesis Report," 2008.
- [30] A. Haddad and D. Warne, "Advances in High Voltage Engineering," *IEE Power & Energy Series 40*. The Institution of Electric Engineers, 2004.
- [31] J. de Urquijo, A. M. Juarez, E. Basurto, and J. L. Hernandez-Avila, "Electron Impact Ionization and Attachment, Drift Velocities and Longitudinal Diffusion in CF₃I and CF₃I-N₂ Mixtures," *Journal of Physics*, vol. D, no. 40, pp. 2205–2209, 2007.
- [32] J. L. Hernandez-Avila, A. M. Juarez, E. Basurto, and J. de Urquijo, "Electron Interactions in CF₃I and CF₃I-N₂," in *XXVIII International Conference on Phenomena in Ionized Gases*, 2007, pp. 139–142.
- [33] J. de Urquijo, "Is CF₃I a good gaseous dielectric? A comparative swarm study of CF₃I and SF₆," *5th EU-Japan Joint Symposium on Plasma Processing*, pp. 1–10, 2007.
- [34] Y.-K. Deng and D.-M. Xiao, "The Effective Ionization Coefficients and Electron Drift Velocities in Gas Mixtures of CF₃I with N₂ and CO₂ obtained from Boltzmann Equation Analysis," *Chinese Physics B*, vol. 22, no. 3, p. 035101, Mar. 2013.
- [35] Y.-Y. Duan, L. Shi, M.-S. Zhu, and L.-Z. Han, "Critical Parameters and Saturated Density of Trifluoroiodomethane (CF₃I)," *Journal of Chemistry & Engineering Data*, vol. 44, pp. 501–504, 1999.

- [36] Y.-Y. Duan, M.-S. Zhu, and L.-Z. Han, "Experimental vapor pressure data and a vapor pressure equation for trifluoroiodomethane (CF₃I)," *Fluid Phase Equilibria*, vol. 121, pp. 227–234, 1996.
- [37] Air Liquide, "Sulfur Hexafluoride Vapor Pressure," 2013. [Online]. Available: http://encyclopedia.airliquide.com/images_encyclopedie/VaporPressureGraph/Sulfur_hexafluoride_Vapor_Pressure.GIF. [Accessed: 13-May-2013].
- [38] Air Liquide, "Carbon Dioxide Vapor Pressure," 2013. [Online]. Available: http://encyclopedia.airliquide.com/images_encyclopedie/VaporPressureGraph/Carbon_dioxide_Vapor_Pressure.GIF. [Accessed: 13-May-2013].
- [39] Air Liquide, "Nitrogen Vapor Pressure," 2013. [Online]. Available: http://encyclopedia.airliquide.com/images_encyclopedie/VaporPressureGraph/nitrogen_vapor_pressure.gif. [Accessed: 13-May-2013].
- [40] H. Katagiri, H. Kasuya, H. Mizoguchi, and S. Yanabu, "Investigation of the Performance of CF₃I Gas as a Possible Substitute for SF₆," *IEEE Transactions on Dielectrics and Electrical Insulation*, vol. 15, no. 5, pp. 1424–1429, 2008.
- [41] H. Kasuya, Y. Kawamura, H. Mizoguchi, Y. Nakamura, and S. Yanabu, "Interruption Capability and Decomposed Gas Density of CF₃I as a Substitute for SF₆ Gas," *IEEE Transactions on Dielectrics and Electrical Insulation*, vol. 17, pp. 1196–1203, 2010.
- [42] H. Kasuya, H. Katagiri, Y. Kawamura, D. Saruhashi, Y. Nakamura, H. Mizoguchi, and S. Yanabu, "Measurement of Decomposed Gas Density of CF₃I-CO₂ Mixture," in *16th International Symposium on High Voltage Engineering*, 2009, pp. 744–747.
- [43] H. Katagiri, H. Kasuya, and S. Yanabu, "Measurement of Iodine Density Generated from CF₃I-CO₂ Mixture after Current Interruption," in *10th Japan-Korea Joint Symposium on Electrical Discharge and High Voltage Engineering*, 2007, pp. 295–298.
- [44] M. Taki, D. Maekawa, H. Odaka, H. Mizoguchi, and S. Yanabu, "Interruption Capability of CF₃I Gas as a Substitution Candidate for SF₆ Gas," *IEEE Transactions on Dielectrics and Electrical Insulation*, vol. 14, no. 2, pp. 341–346, 2007.
- [45] European Committee for Electrotechnical Standardization, "BS EN 60060-1 : 2010 BSI Standards Publication High-voltage test techniques Part 1 : General definitions and test requirements," 2010.
- [46] H. Toyota, S. Nakauchi, S. Matsuoka, and K. Hidaka, "Voltage-time Characteristics in SF₆ and CF₃I Gas within Non-uniform Electric Field," in *Proceedings of the 14th International Symposium on High Voltage Engineering*, 2005, p. 466.

- [47] T. Takeda, S. Matsuoka, A. Kumada, and K. Hidaka, "Sparkover and Surface Flashover Characteristics of CF₃I Gas under Application of Nanosecond Square Pulse Voltage," in *16th International Symposium on High Voltage Engineering*, 2009, pp. 812–817.
- [48] H. Anis and K. Srivastava, "Pre-Breakdown Discharges in Highly Non-Uniform Fields in Relation to Gas-Insulated Systems," *IEEE Transactions on Electrical Insulation*, vol. EI-17, no. 2, pp. 131–142, Apr. 1982.
- [49] H. Toyota, S. Matsuoka, and K. Hidaka, "Measurement of Sparkover Voltage and Time Lag Characteristics in CF₃I-N₂ and CF₃I-Air Gas Mixtures by using Steep-Front Square Voltage," *Electrical Engineering in Japan*, vol. 157, no. 2, pp. 1–7, 2006.
- [50] T. Takeda, S. Matsuoka, A. Kumada, and K. Hidaka, "Insulation Performance of CF₃I and Its By-Products by Spark-over Discharge," in *International Conference on Electrical Engineering*, 2008, pp. 1–6.
- [51] T. Takeda, S. Matsuoka, A. Kumada, and K. Hidaka, "Breakdown Characteristics of CF₃I Gas in Uniform and Non-Uniform Field Gap Under Various Voltage Applications of Nanosecond Pulse to AC," in *Fifteenth International Symposium on High Voltage Engineering*, 2007, pp. 7–10.
- [52] S. Nakauchi, D. Tosu, S. Matsuoka, A. Kumada, and K. Hidaka, "Breakdown Characteristics Measurement of Non-uniform Field Gap in SF₆/N₂, CF₃I/N₂ and CF₃I/CO₂ Gas Mixtures by Using Square Pulse Voltage," in *The XVI International Conference on Gas Discharge and Their Applications*, 2006, vol. 2, pp. 365–368.
- [53] H. Toyota, S. Matsuoka, and K. Hidaka, "Voltage-Time Characteristics of SF₆-N₂ and CF₃I-N₂ Gas Mixtures in Nanosecond Range," in *The XV International Conference on Gas Discharge and Their Applications*, 2004, no. September, pp. 395–398.
- [54] H. Katagiri, H. Kasuya, H. Mizoguchi, and S. Yanabu, "BTF Interruption Capability of CF₃I-CO₂ Mixture," in *Proceedings of XVII International Conference on Gas Discharges and Their Applications*, 2008, pp. 105–108.
- [55] T. Takeda, S. Matsuoka, A. Kumada, and K. Hidaka, "Flashover Characteristics of CF₃I on the Dielectric Surface," in *Proceedings of XVIII International Conference on Gas Discharges and Their Applications*, 2010, pp. 268–271.
- [56] M. Dayah, "Dynamic Periodic Table," 1997. [Online]. Available: <http://www.ptable.com/>. [Accessed: 05-Jun-2013].
- [57] T. Takeda, S. Matsuoka, A. Kumada, and K. Hidaka, "By-products of CF₃I produced by Spark Discharge," in *10th Japan-Korea Joint Symposium on Electrical Discharge and High Voltage Engineering*, 2007, pp. 157–160.

- [58] M. Kamarol, Y. Nakayama, T. Hara, S. Ohtsuka, and M. Hikita, "Gas Decomposition Analysis of CF₃I under AC Partial Discharge of Non-Uniform Electric Field Configuration," in *10th Japan-Korea Joint Symposium on Electrical Discharge and High Voltage Engineering*, 2007, pp. 161–164.
- [59] S. M. Webb, D. Jaksch, R. a. McPheat, E. Drage, E. Vasekova, P. Limão-Vieira, N. J. Mason, and K. M. Smith, "High-Resolution, Temperature Dependant, Fourier Transform Infrared Spectroscopy of CF₃I," *Journal of Quantitative Spectroscopy and Radiative Transfer*, vol. 94, no. 3–4, pp. 425–438, Sep. 2005.
- [60] T. Takeda, S. Matsuoka, A. Kumada, and K. Hidaka, "Breakdown Characteristics of CF₃I on Dielectric Surface," in *2009 Korea-Japan Joint Symposium on Electrical Discharge and High Voltage Engineering*, 2009, pp. 104–107.
- [61] M. N. Ngoc, A. Denat, N. Bonifaci, O. Lesaint, W. Daoud, and M. Hassanzadeh, "Electrical breakdown of CF₃I and CF₃I-N₂ gas mixtures," in *IEEE Conference on Electrical Insulation and Dielectric Phenomena*, 2009, pp. 557–560.
- [62] N. M. Nguyen, A. Denat, N. Bonifaci, O. Lesaint, and M. Hassanzadeh, "Impulse Partial Discharges and Breakdown of CF₃I in Highly Non-Uniform Field," in *Eighteenth International Conference on Gas Discharges and Their Applications*, 2010, pp. 330–333.
- [63] L. L. Burger and R. D. Scheele, "HWVP Iodine Trap Evaluation," Pacific Northwest National Laboratory, 2004.
- [64] Sigma-Aldrich Co., "Sigma-Aldrich United Kingdom," 2013. .
- [65] Sigma-Aldrich Co., "Pentafluoroiodoethane Safety Data Sheet," 2012.
- [66] Sigma-Aldrich Co., "Hexafluoroethane Safety Data Sheet," 2012.
- [67] Sigma-Aldrich Co., "Hexafluoropropene Safety Data Sheet," 2012.
- [68] Sigma-Aldrich Co., "Trifluoroiodomethane Safety Data Sheet," 2012.
- [69] Sigma-Aldrich Co., "Trifluoromethane Safety Data Sheet," 2012.
- [70] Sigma-Aldrich Co., "Carbon Dioxide Safety Data Sheet," 2012.
- [71] Sigma-Aldrich Co., "Sulfur Hexafluoride Safety Data Sheet," 2012.
- [72] Sigma-Aldrich Co., "Air Safety Data Sheet," 2012.
- [73] European Standard, "European Structural Steel Standard EN 10024-2 : 2004," *Grade designations, properties and nearest equivalent*. Corus UK Ltd., 2004.
- [74] PlasticsEurope, "The Plastic Portal - Polycarbonate," 2010. [Online]. Available: <http://www.plasticseurope.org/what-is-plastic/types-of-plastics/polycarbonate.aspx>. [Accessed: 17-Jun-2013].

- [75] HighLine Polycarbonate, “FDA and NSF Standard 51 Grades and UV Absorbers,” 2011. [Online]. Available: <http://highlinepc.blogspot.co.uk/2011/05/fda-and-nsf-standard-51-grades-and-uv.html>. [Accessed: 20-Sep-2013].
- [76] City Plastics, “Polycarbonate Technical Data and Information Sheet,” 2005.
- [77] Copper Development Association, “Types of Brass,” 2012.
- [78] CCOHS, “Non-Sparking Tools : OSH Answers.” [Online]. Available: http://www.ccohs.ca/oshanswers/safety_haz/hand_tools/nonsparking.html. [Accessed: 07-May-2013].
- [79] Firgelli Technologies Inc., “Miniature Linear Motion Series • L12,” vol. 1, no. 206, 2008.
- [80] Phidgets Inc., “Product Manual 1066 - PhidgetAdvancedServo 1-Motor,” 2009.
- [81] ANSI/IEEE, “IEEE Standard General Requirements and Test Procedure for Outdoor Apparatus Bushings,” 1976.
- [82] International Electrotechnical Commission, “IEC 60137 - Insulated Bushing for Alternating Voltages Above 1000 V,” 2003.
- [83] Oregon Scientific, “Advanced Weather Station with Atomic Time Model : BAR208HGA USER MANUAL,” pp. 3–4, 2000.
- [84] Concept Engineering Ltd, “Concept CO₂ Heater,” 2000. [Online]. Available: http://www.concept-smoke.co.uk/concept_co2_heater_for_vicount_vulcan_smoke_generators.aspx. [Accessed: 06-Jun-2013].
- [85] DILO Armaturen und Anlagen GmbH, *Operating Manual for Z579R03*, vol. 0, no. 49. 2012.
- [86] S. Ohtsuka, M. Koumura, M. Cho, Y. Hashimoto, M. Nakamura, and M. Hikita, “Insulation Properties of CO₂/N₂ Gas Mixture with a Small Amount of SF₆,” in *Gaseous Dielectrics IX*, Springer US, 2001, pp. 295–300.
- [87] J. Wolf, *Manual Instruction of Impulse Voltage Generator Type SGS*. Haefely Test AG, 2002.
- [88] J. Wolf, *Manual Instructions of the Charging Rectifier*. Haefely Test AG, 1998.
- [89] J. H. Cloete and J. van der Merwe, “The Breakdown Electric Field between Two Conducting Spheres by the Method of Images,” *IEEE Transactions on Education*, vol. 41, no. 2, pp. 141–145, May 1998.
- [90] P. G. Slade and E. D. Taylor, “Electrical Breakdown in Atmospheric Air Between Closely Spaced (0.2pm-40pm) Electrical Contacts,” in *Proceedings of*

the Forty-Seventh IEEE Holm Conference on Electrical Contacts, 2001, pp. 245–250.

- [91] K. J. Bathe, *Finite Element Procedures*. Prentice Hall, 2006.
- [92] P. B. Zhou, *Numerical Analysis of Electromagnetic Fields*. Berlin: Springer-Verlag, 1993.
- [93] E. Kuffel and W. S. Zaengl, “Finite Element Method (FEM),” in in *High Voltage Engineering: Fundamentals*, 1st ed., Pergamon Press, 1984, pp. 266–279.
- [94] R. N. Clarke and National Physics Laboratory, “Dielectric Properties of Materials,” 2013. [Online]. Available: http://www.kayelaby.npl.co.uk/general_physics/2_6/2_6_5.html. [Accessed: 17-May-2013].
- [95] S. Kasap, *Dielectric Materials: Relative Permittivity*, no. 2. Web-Materials, 2002, pp. 1–7.
- [96] R. Kurtus, “Polar and Non-Polar Molecules,” *School of Champions*, 2005. [Online]. Available: http://www.school-for-champions.com/chemistry/polar_molecules.htm. [Accessed: 17-May-2013].
- [97] COMSOL, *AC/DC Module User’s Guide*. COMSOL, 2012.
- [98] E. Husain and R. S. Nema, “Analysis of Paschen Curves for Air, N₂, and SF₆ using the Townsend Breakdown Equation,” *IEEE Transactions on Electrical Insulation*, vol. EI-17, no. August, pp. 4–7, 1982.
- [99] G. R. Govinda Raju and R. Hackam, “Sparking Potentials of Dry Air, Humid Air and Water Vapour between Concentric Sphere-Hemisphere Electrodes,” *Proceedings of IEE*, vol. 120, no. August, pp. 927–933, 1973.
- [100] J. Lux, “Pachen’s Law,” *High Voltage Experimenter’s Handbook*, 2004. [Online]. Available: <http://home.earthlink.net/~jimlux/hv/paschen.htm>. [Accessed: 28-Jul-2013].
- [101] M. S. Naidu and V. Kamaraju, “Paschen’s Law,” in in *High Voltage Engineering*, 4th ed., Tata McGraw-Hill, 2009, pp. 45–48.
- [102] P. N. Mavroidis, P. N. Mikropoulos, and C. a. Stassinopoulos, “Discharge Characteristics in Short Rod-Plane Gaps under Lightning Impulse Voltages of Both Polarities,” in *42nd International Universities Power Engineering Conference*, 2007, pp. 1070–1074.
- [103] A. E. D. Heylen, “Sparking formulae for very high-voltage Paschen characteristics of gases,” *IEEE Electrical Insulation Magazine*, vol. 22, no. 3, pp. 25–35, May 2006.

- [104] J. S. Pearson and J. A. Harrison, "A Uniform Field Electrode for use in a Discharge Chamber of Restricted Size: Design and Performance," *Journal of Physics D: Applied Physics*, vol. 2, no. 1, pp. 77–84, 1969.
- [105] S.-Y. Woo, D.-H. Jeong, K.-B. Seo, and J.-H. Kim, "A Study on Dielectric Strength and Insulation Property of SF₆/N₂ Mixtures for GIS," *Journal of International Council on Electrical Engineering*, vol. 2, no. 1, pp. 104–109, 2012.
- [106] E. Kuffel and W. S. Zaengl, "Fields in Homogeneous, Isotropic Materials," in in *High Voltage Engineering: Fundamentals*, 1st ed., Pergamon Press, 1984, pp. 224–232.
- [107] P. R. Howard, "Process Contributing to the Breakdown of Electronegative Gases in Uniform and Non-Uniform Electric Fields," *Proceedings of the IEE - Part A: Power Engineering*, vol. 104, no. 14, pp. 139–142, 1957.
- [108] W. D. Greason, Z. Kucerovsky, S. Bulach, and M. W. Flatley, "Investigation of the Optical and Electrical Characteristics of a Spark Gap," *IEEE Transactions on Industry Applications*, vol. 33, no. 6, pp. 1519–1526, 1997.
- [109] T. Takuma, "Discharge Characteristics of Gaseous Dielectrics," *IEEE Transactions on Electrical Insulation*, vol. EI-21, no. 6, 1986.
- [110] Y. Hoshina, M. Sato, M. Shiiki, M. Hanai, and E. Kaneko, "Lightning Impulse Breakdown Characteristics of SF₆ Alternative Gases for Gas-Insulated Switchgear," *IEE Proceedings - Science, Measurement and Technology*, vol. 153, no. 1, pp. 1–6, 2006.
- [111] C. Jones, "Future Trends of Gas Insulated Substations," in in *Gaseous Dielectrics X*, L. G. Christophorou, J. K. Olthoff, and P. Vassiliou, Eds. New York: Springer Science + Business Media, Inc., 2004, pp. 375–384.
- [112] L. B. Loeb and A. F. Kip, "Electrical Discharges in Air at Atmospheric Pressure - The Nature of the Positive and Negative Point-to-Plane Coronas and the Mechanism of Spark Propagation," *Journal of Applied Physics*, vol. 10, no. 3, pp. 142–160, 1939.
- [113] C. N. Works and T. W. Dakin, "Dielectric Breakdown of Sulfur Hexafluoride in Nonuniform Fields," *Transactions of the American Institute of Electrical Engineers*, vol. 72, no. 5, pp. 682–689, 1953.
- [114] L. Nierneyer, L. Ullrich, and N. Wiegart, "The Mechanism of Leader Breakdown in Electronegative Gases," *IEEE Transactions on Electrical Insulation*, vol. 24, no. 2, pp. 309–324, 1989.
- [115] A. H. Sharbaugh and P. K. Watson, "Breakdown Strengths of a Perfluorocarbon Vapor (FC-75) and Mixtures of the Vapor with SF₆," *IEEE Transactions on Power Apparatus and Systems*, vol. 83, no. 2, pp. 131–136, 1964.

- [116] M. J. Mulcahy, "Electrical Breakdown of Air and SF₆ Mixtures," *Proceedings of the Institution of Electrical Engineers*, vol. 113, no. 11, pp. 1878–1880, 1966.
- [117] S. J. MacGregor, I. D. Chalmers, and G. Street, "The Switching Properties of SF₆ Gas Mixtures," in *Pulsed Power Conference*, 1989, pp. 510–513.
- [118] Elimsan Group, "SF₆ Gas Circuit Breakers."
- [119] ABB Limited, "Indoor Live Tank SF₆ Circuit Breaker," 2009.
- [120] T. Yoshida, H. Fujinami, and T. Kawamoto, "V-t Characteristics of SF₆ Gas during Lightning Surges," *Electrical Engineering in Japan*, vol. 119, no. 4, pp. 1232–1239, 1997.
- [121] O. Yamamoto, T. Takuma, S. Hamada, and Y. Yamakawa, "Applying a Gas Mixture Containing c-C₄F₈ as an Insulation Medium," *IEEE Transactions on Dielectrics and Electrical Insulation*, vol. 8, no. 6, pp. 1075–1081, 2001.
- [122] W. Xing, G. Zhang, K. Li, W. Niu, X. Wang, and Y. Wang, "Experimental Study on Partial Discharge Characteristics of C₄F₈-N₂ Mixtures," *Proceedings of the Chinese Society for Electrical Engineering*, vol. 31, no. 7, pp. 119–124, 2011.
- [123] K. Yanallah and F. Pontiga, "A Semi-Analytical Stationary Model of a Point-to-Plane Corona Discharge," *Plasma Sources Science and Technology*, vol. 21, no. 4, 2012.
- [124] D. McMullan, "Scanning Electron Microscopy," 1993. [Online]. Available: <http://www-g.eng.cam.ac.uk/125/achievements/mcmullan/mcm.htm>. [Accessed: 31-May-2013].
- [125] J. Atteberry, "How Scanning Electron Microscopes Work," *HowStuffWorks.com*, 2009. [Online]. Available: <http://science.howstuffworks.com/scanning-electron-microscope.htm>. [Accessed: 31-May-2013].
- [126] Central Facility for Advanced Microscopy and Microanalysis, "Introduction to Energy Dispersive X-ray Spectrometry (EDS)," 1996.